HHS Public Access

Author manuscript

Cell Rep. Author manuscript; available in PMC 2017 August 19.

Published in final edited form as:

Cell Rep. 2017 April 04; 19(1): 86–100. doi:10.1016/j.celrep.2017.03.028.

Retrogradely trafficked TrkA endosomes signal locally within dendrites to maintain sympathetic neuron synapses

Kathryn M. Lehigh[1,2], **Katherine M. West**[1], and **David D. Ginty**[1,3]

[1]Department of Neurobiology, Howard Hughes Medical Institute, Harvard Medical School, 220 Longwood Avenue, Boston, MA 02115, USA

[2]Neuroscience Training Program, Department of Neuroscience, The Johns Hopkins University, School of Medicine, Baltimore, MD 21205, USA

Summary

Sympathetic neurons require NGF from their target fields for survival, axonal target innervation, dendritic growth and formation, and maintenance of synaptic inputs from preganglionic neurons. Target-derived NGF signals are propagated retrogradely, from distal axons to somata of sympathetic neurons via TrkA signaling endosomes. We report that a subset of TrkA endosomes that are transported from distal axons to cell bodies also translocate into dendrites, where they are signaling-competent and move bidirectionally, in close proximity to synaptic protein clusters. Using a strategy for spatially-confined inhibition of TrkA kinase activity, we found that distal axon-derived TrkA signaling endosomes are necessary specifically within sympathetic neuron dendrites for maintenance of synapses. Thus, TrkA signaling endosomes have unique functions in different cellular compartments. Moreover, target-derived NGF mediates circuit formation and synapse maintenance through TrkA endosome signaling within dendrites to promote aggregation of postsynaptic protein complexes.

Introduction

Development of nervous system connectivity involves the orchestration of several events: axons are guided to their targets, axons and dendrites elaborate and form synaptic connections, and excess or improper synaptic connections are pruned (Jiang and Nardelli, 2016). A useful model system for studying the development of neural connectivity has been the sympathetic nervous system (SNS) because it is easily accessible and has well defined anatomy: preganglionic sympathetic neurons are located in the intermediolateral region of the spinal cord; their axons exit the spinal cord via ventral roots and project to sympathetic

Correspondence: david_ginty@hms.harvard.edu.
[3]Lead Contact

Supplemental Information

Supplemental Information includes Supplemental Experimental Procedures, five movies and six figures.

Author Contributions

K.M.L. and D.D.G. conceived the study. K.M.L. developed the Flag-TrkA live cell imaging assay, use of 1NMPP1 loaded microspheres for both SCG injection assay and local dendritic inhibition assay, and performed all experiments and analysis, with assistance from K.M.W. for genotyping, tissue preparation, IHC, and image analysis. K.M.L. and D.D.G. wrote the paper with editing from K.M.W.

ganglia where they form synapses upon dendrites of postganglionic sympathetic neurons. As the SNS is a major regulator of body homeostasis, disruption of SNS circuits causes several human pathological conditions. For example, Horner's syndrome, a disorder affecting the rostral-most ganglion of the sympathetic chain, the superior cervical ganglion (SCG), is caused by an interruption of SCG connectivity. Consequently, Horner's syndrome patients exhibit miosis, ptosis, and anhidrosis (Fields and Barker, 1992). Investigations of how SNS synapses are formed and maintained will reveal mechanisms that underlie SNS disorders such as Horner's syndrome.

Nerve growth factor (NGF), the prototypical neurotrophin, is essential for development and maintenance of sympathetic neurons. Seminal work from Levi-Montalcini and colleagues showed that NGF mediates survival of sympathetic neurons (Levi-Montalcini and Booker, 1960) while later work demonstrated that NGF also controls sympathetic neuron target field innervation, dendrite elaboration, and formation and maintenance of synapses with preganglionic partners (Glebova and Ginty, 2004; Nja and Purves, 1978; Ruit et al., 1990; Ruit and Snider, 1991; Sharma et al., 2010). How NGF derived from sympathetic neuron target fields promotes and maintains synaptic connections between preganglionic and postganglionic sympathetic neurons remains to be determined.

Considerable evidence supports a model in which NGF/TrkA signaling endosomes mediate long-range retrograde signaling to promote sympathetic neuron survival. NGF is produced in sympathetic target tissues throughout development and adulthood (Heumann et al., 1984; Sofroniew et al., 2001), where it binds to its receptor, the tyrosine kinase TrkA, initiating endocytosis of the ligand and receptor complex at distal axons followed by retrograde transport of NGF/TrkA endosomes to cell bodies (Riccio et al., 1997; Tsui-Pierchala and Ginty, 1999; Watson et al., 1999). Application of NGF to distal axons of neurons grown in compartmentalized cultures supports cell survival (Campenot, 1977) as well as TrkA signaling within cell bodies (Riccio et al., 1997; Senger and Campenot, 1997; Tsui-Pierchala and Ginty, 1999; Watson et al., 1999), which in turn is required for activation of NGF/TrkA signaling effectors that promote survival (Kuruvilla et al., 2000; Riccio et al., 1997; Ye et al., 2003). Furthermore, disruption of TrkA signaling and downstream effectors in cell bodies of sympathetic neurons following NGF application to distal axons results in cell death (Kuruvilla et al., 2000; Kuruvilla et al., 2004; Ye et al., 2003). Together, these findings support a model in which signals emanating from distal-axon derived NGF/TrkA endosomes within cell bodies are required for survival of sympathetic neurons. Interestingly, NGF acting exclusively on distal axons of cultured sympathetic neurons can also support the formation of clusters of post-synaptic density (PSD) proteins on dendrites (Sharma et al., 2010). Under these conditions, inhibition of TrkA signaling within the somatodendritic compartment of cultured neurons leads to loss of PSD clusters. These observations raise the intriguing possibility that TrkA endosomes may traffic from distal axons, where they are formed, into the cell soma and then into dendrites where they signal locally, within dendrites, to promote formation and maintenance of synapses between preganglionic and postganglionic sympathetic neurons.

Here, we report that TrkA endosomes originating in sympathetic neuron distal axons are transported retrogradely into dendrites as signaling competent entities that move in a unique,

bidirectional manner, as compared to TrkA endosomes in axons, and in close proximity to PSD clusters. We also find signaling competent TrkA endosomes within sympathetic neuron dendrites *in vivo*, adjacent to synapses, at both early and late stages of dendrite development and synapse formation. Importantly, we show that TrkA kinase activity within the SCG is essential for the maintenance of synapses between preganglionic and postganglionic sympathetic neurons *in vivo.* Moreover, distal axon-derived TrkA signaling endosomes function within dendrites, not cell bodies, for maintenance of dendritic PSD clusters *in vitro.* Thus, target-derived NGF supports synapse formation and maintenance through local TrkA endosome signaling within sympathetic neuron dendrites.

Results

Live cell imaging of TrkA endosomes reveals unique dynamics in different cellular compartments

The observation that distal axon-derived TrkA endosomes are transported from the soma into the dendrites of sympathetic neurons (Sharma et al., 2010) suggests novel TrkA signaling functions within that cellular compartment. To gain insight into TrkA endosome function in dendrites, we first sought to characterize TrkA endosome dynamics within dendrites and their location, with respect to dendritic PSDs. To monitor TrkA endosome dynamics, we developed a live cell imaging paradigm that enables visualization of TrkA endosomes in real time, thus providing a means to compare their movement in axons, cell bodies, and dendrites. This live cell imaging paradigm involves culturing dissociated postganglionic sympathetic neurons obtained from the $TrkA^{Flag}$ mouse line, which expresses Flag epitope-tagged TrkA protein from the endogenous *TrkA* locus (Sharma et al., 2010), in microfluidic chambers (Taylor et al., 2010). Addition of an anti-Flag primary and fluorescent secondary antibody conjugate, followed by application of NGF, to the distal axon compartment, allows for real-time visualization of newly internalized TrkA endosomes as they are retrogradely trafficked from distal axons into cell bodies and dendrites (Figure 1A and Movies S1–5). Importantly, fluorescent puncta were not observed in control, wild-type neurons, indicating that the Flag and fluorescent secondary antibody combination specifically recognizes Flag-TrkA in $TrkA^{Flag}$ neurons (Figure 1B).

Using this live cell TrkA imaging assay, we found that TrkA endosomes move in a saltatory manner retrogradely through axons (Figure 1C, E and Movie S1) with highly variable rates, averaging 1.22 ± 0.23 μm/s (Figures 2A, S1B–C), which is similar to the rate of retrograde axonal transport of its ligand, NGF (Cui et al., 2007; Hendry et al., 1974). TrkA endosomes in axons move exclusively in a retrograde manner, from distal axons to cell bodies (Figure 2C and Movies S1, 3–4). This is expected because trafficking of NGF-containing endosomes in axons is dependent on the retrograde motor protein dynein (Heerssen et al., 2004). We noted that TrkA endosomes in the same axon frequently paused at similar or identical locations (Movie S1, 3–4). Faster endosomes more quickly traversed the length of the axon while slower endosomes more typically exhibited frequent pauses or became stationary for the duration of the recording (Figures 1E, S1C and Movie S1).

We observed that TrkA endosomes retrogradely trafficked from distal axons first arrive in cell bodies between 15 and 30 minutes following NGF application to distal axons (data not

shown). Upon arrival in the soma, labeled endosomes slow down or halt, resulting in their accumulation within cell bodies (Movies S2–5). We photobleached accumulated endosomes within the soma to monitor movement of endosomes that were newly transported from the axon into the soma, and this revealed that TrkA endosomes within the soma move at an average rate of 0.14 ±0.02 μm/s (Figure 2A). Many somatic endosomes were localized to a perinuclear region where they did not exhibit appreciable movement (Figure S1A).

Peripherally located somatic endosomes were often observed moving from cell body to dendrites after minor pauses (Movie S3). We determined that 4.2% ± 0.3% of TrkA endosomes in the somatodendritic compartment three hours after NGF application to distal axons were in dendrites. Thus, we next used the live cell TrkA endosome assay to monitor TrkA endosome movement within dendrites (DIV 14–16), the identity of which was confirmed by post hoc MAP2 immunocytochemistry (ICC) (Figure 1G). We observed that distal axon-derived TrkA endosomes within dendrites move in a bidirectional manner (Figure 1D, F and Movies S4–5), representing a fundamental difference from the manner in which TrkA endosomes travel within axons (Figure 2C and Movie S5). Although dendritic TrkA endosomes are capable of moving at rates that are comparable to those in axons (Figure S1B), their unique dynamics (i.e. frequent direction changes and oscillatory movements) result in an overall lower average rate of movement (Figure 2A) and a lower net displacement as a function of time compared to endosomes in axons (Figure 2B). This distinction is readily appreciated upon visualization of dendritic TrkA endosome dynamics in real time as they tend to hover around small regions of dendrite, in contrast to the much longer distances covered by TrkA endosomes in axons (Figure 1E–F and Movies S4–5). Further, we observed a substantial subset (~20%) of distal axon-derived Flag-TrkA endosomes within dendrites that remain stationary (Figure 1F and Movies S4–5). However, this is not the fate of the majority of dendritic TrkA endosomes, which maintain mobility (Figure 2D) and even return to the soma (Movie S5). These experiments show that the dynamics of movement of distal axon-derived TrkA endosomes differ markedly within cellular compartments.

Distal axon-derived TrkA endosomes in dendrites are signaling competent and located near PSDs

The current view of NGF signal transduction is that TrkA endosomes carry critical retrograde signals from the periphery to cell bodies of sympathetic neurons (Barford et al., 2016; Harrington et al., 2011). Therefore, we asked whether TrkA endosomes that traffic into dendrites are signaling competent. TrkA kinase activation results in autophosphorylation of specific TrkA tyrosine (Y) residues, including Y490 and Y785. Once phosphorylated, these TrkA phosphotyrosine motifs recruit adaptor and effector complexes to the membrane to promote downstream NGF/TrkA signaling pathways, including the Ras/ERK, PI3 kinase, and PLCγ pathways (Barford et al., 2016). Therefore, we used antibodies directed against the phosphorylated forms of TrkA Y490 and Y785 (Huang et al., 2015) to assess the extent to which TrkA endosomes in dendrites are signaling competent.

First, specificity of the TrkA Y490 and Y785 antibodies in this paradigm was tested using a chemical genetic strategy with compartmentalized cultures of sympathetic neurons from

TrkA^{F592A} mice. *TrkA*^{F592A} mice harbor a single phenylalanine-to-alanine amino acid substitution in the TrkA protein kinase domain, which allows TrkA^{F592A}, but not wild-type TrkA, catalytic activity to be selectively blocked by the membrane permeable small molecule 1NMPP1 (Chen et al., 2005), thereby providing a means of selective inhibition of TrkA autophosphorylation and signaling. Indeed, we observed nearly complete loss of P-TrkA (Y490) and P-TrkA (Y785) immunoreactivity in *TrkA*^{F592A} neurons treated with 1NMPP1 but no change in the number of P-TrkA puncta in 1NMPP1 treated wild-type neurons (Figures 3A, S2A–D). We conclude that the antibodies directed against the phosphorylated forms of TrkA Y490 and Y785 specifically label these phospho-TrkA motifs in our ICC experiments.

Next, we used these specific phospho-TrkA antibodies to ask if distal-axon derived TrkA endosomes in dendrites are signaling competent by performing P-TrkA staining on compartmentalized *TrkA*^{Flag} neurons after NGF application to distal axons. Following a 2–4 hour incubation period to allow accumulation of retrogradely transported Flag-TrkA endosomes and P-TrkA puncta within dendrites, ~34% of Flag-TrkA endosomes in dendrites were found to be P-TrkA (Y785) positive and ~15% were P-TrkA (Y490) positive (Figure 3B–D) at this time point. Flag-TrkA endosomes that are not P-TrkA (Y785) or P-TrkA (Y490) positive may represent TrkA endosomes returning to the cell body or endosomes on the pathway to lysosomal degradation (Hu et al., 2015). Conversely, P-TrkA endosomes that are not Flag-TrkA positive likely represent NGF activated TrkA not bound by Flag antibody during the pulse application of Flag antibody to distal axons.

The presence of signaling-competent TrkA endosomes in dendrites lends support to the idea that distal axon-derived TrkA endosomes within dendrites contribute to synapse formation and/or maintenance. To explore the relationship between TrkA endosomes and dendritic synapses, we determined the extent to which dendritic TrkA endosomes derived from distal axons are localized in close proximity to PSDs. Following NGF application solely to distal axons of sympathetic neurons, Flag-TrkA endosomes were often observed adjacent to MAGUK positive PSDs throughout the dendritic arbor (Figure 3E). In the same experimental paradigm, double labeling ICC experiments revealed a non-random, close spatial relationship, with some co-localization, between P-TrkA (Y785) signaling competent endosomes and PSDs labeled with both MAGUK (Figure 3F–H) and Homer1 (Figure S2E). A nearest neighbor analysis comparing the spatial relationship between the different puncta types showed that the proximity of signaling competent TrkA endosomes (P-TrkA (Y785) puncta) to MAGUK puncta is considerably closer than what would be expected by chance alone (Figures 3G–H, S2F–G). This intimate spatial relationship between TrkA endosomes and PSDs within dendrites suggests that distal-axon derived TrkA signaling endosomes are poised to promote or maintain PSD component clustering or function.

Distal axon-derived endosomes are signaling competent in dendrites of postganglionic neurons in sympathetic ganglia *in vivo*

We next sought to determine whether distal axon-derived TrkA endosomes are trafficked into sympathetic neuron dendrites *in vivo.* To this end, we analyzed endosomes derived from sympathetic neuron axonal terminals innervating the eye, a major target of the superior

cervical ganglion (SCG). Injection of fluorescently-conjugated Wheat Germ Agglutinin (WGA) into the anterior chamber of the eye resulted in its uptake into endosomes at sympathetic neuron distal axons and retrograde transport within sympathetic neuron axons, into cell bodies of the SCG and ultimately into SCG sympathetic neuron dendrites (Figure 4A–D). WGA containing endosomes were confined to the ganglion ipsilateral to the injected anterior chamber, and not present in the contralateral ganglion (Figure 4B). Because sympathetic neurons project exclusively to ipsilateral targets, this finding indicates that uptake and transport occurs from the target region via sympathetic neuron axons (Figure 4C) and not via leak into the circulatory system, which would be expected to result in direct uptake at the soma of both ipsilateral and contralateral ganglia. The appearance of WGA vesicles in both soma and dendrites of neurons in the ipsilateral ganglion occurred within 16 hours post injection (Figure 4D), consistent with the previously described timing of retrograde transport of NGF from distal target innervating axonal terminals to SCG cell bodies (Hendry et al., 1974). To ask if $TrkA^{Flag}$ receptors endocytosed at the distal axon were transported into dendrites, we performed the WGA eye injection assay on adult $TrkA^{Flag}$ mice and indeed observed that endosomes with retrogradely-transported WGA protein co-localized with Flag-TrkA labeled puncta in neuronal dendrites (Figure 4E, G). We confirmed that Flag staining in SCG tissue is specific to $TrkA^{Flag}$ mice, observing no labeled puncta in wild-type animals (Figure 4H). These observations support the idea that TrkA endosomes are trafficked retrogradely from sympathetic axon terminals into SCG dendrites *in vivo.*

We next asked whether target-derived TrkA endosomes observed *in vivo* are signaling competent by combining the WGA eye injection retrograde tracing assay with P-TrkA (Y785) immunohistochemistry (IHC). Indeed, as the *in vitro* findings suggested, co-localization between WGA positive vesicles and P-TrkA positive puncta was observed (Figure 4F–G). The number of WGA vesicles transported into dendrites was not significantly different for Flag-TrkA or P-TrkA experiments (Figure S3C). Moreover, the specificity of the P-TrkA antibody in these *in vivo* experiments was confirmed using chemical-genetic $TrkA^{F592A}$ mice (Figures 4I, S3A–B). Thus, TrkA endosomes found in dendrites of sympathetic neurons are derived from distal axons and signaling competent.

Signaling competent endosomes are found within dendrites and in close proximity to SCG neuron synapses throughout development

If retrogradely transported NGF-TrkA endosomes signal locally within dendrites to promote formation and maintenance of synaptic connectivity, then we would expect to find signaling-competent endosomes within dendrites of sympathetic neurons not only throughout the period of robust synapse development but later as well. Utilizing $TH^{2a\text{-}CreER}$; $R26^{LSL\text{-}YFP}$ (Ai3) mice (Abraira et al., 2017) and postnatal tamoxifen injection to achieve sparse genetic labeling of sympathetic neurons and their dendrites within the SCG (Figure S4A–B), we observed the presence of P-TrkA (Y785) puncta associated with sympathetic neuron dendrites at all examined postnatal (P) ages: P7, P14, P21, and P42–P56 (Figure 5A). We note that both the number of P-TrkA (Y785) puncta (Figure 5B) and the number of synapses (immunohistochemically defined as Homer1-VAChT double positive puncta) within dendrites increase between developmental (P14) and young adult (P42–P56) ages (Figures

5C, S4C). These findings suggest that TrkA signals are propagated within dendrites during the most robust stages of dendritic growth (Voyvodic, 1987) and synapse formation (Smolen and Raisman, 1980) as well as during periods of final synapse formation (Smolen and Raisman, 1980), maturation and maintenance (Heath et al., 1992).

Our *in vitro* findings revealed a close spatial relationship between TrkA signaling endosomes and synaptic proteins, so we examined this *in vivo* as well. Indeed, we found that P-TrkA (Y785) puncta within sympathetic neuron dendrites are in close proximity to pre-synaptic cholinergic terminals of preganglionic sympathetic neurons as measured by VAChT labeling (Figure 5A). Interestingly, the percentage of P-TrkA endosomes that were within 1μm of a VAChT punctum increased from ~30% at early developmental stages (P7–P14) to ~45% at later stages (P21–P56). A similar increase was observed with pre- and postsynaptic proteins; the percentage of Homer1 puncta located within 1μm of a VAChT punctum increased from ~50% to ~80% during this period (Figure 5D–E). Together, these findings suggest that distal axon-derived TrkA endosomes are trafficked into dendrites both *in vitro* and *in vivo*, where they are signaling competent and located in close proximity to nascent synapses.

Inhibition of TrkA kinase activity selectively within the SCG decreases synapse number and function

Our findings, together with previous observations (Sharma et al., 2010) support a model in which dendritic TrkA endosomes function within the somatodendritic compartment, and possibly within dendrites themselves, to promote synapse formation and maintenance. To test this model, we asked whether inhibiting TrkA kinase activity selectively within the ganglion, but not in distal axons, would alter the number of dendritic synapses found at P21, an age at which postganglionic sympathetic neuron dendrites are elaborate with an abundance of mature synapses, yet new synapses continue to develop (Figure 5C) (Smolen and Raisman, 1980; Voyvodic, 1987). As previously demonstrated, TrkA kinase activity can be specifically and efficiently inhibited in $TrkA^{F592A}$ mice by administering 1NMPP1, and the extent and localization of TrkA inhibition can be monitored by IHC using the specific P-TrkA (Y785) antibody (Figures 3A, 4I). To restrict inhibition of TrkA signaling to the somatodendritic compartment of SCG neurons we developed a procedure in which 1NMPP1 incorporated into Poly-Lactic-co-Glycolic-Acid (PLGA) microspheres is injected directly into the SCG (Figure 6A). PLGA microspheres are a biodegradable drug delivery vehicle that release incorporated molecules as they undergo hydrolysis in aqueous environments (Makadia and Siegel, 2011) and are thus ideal for sustained and local 1NMPP1 release. To ensure specificity of the approach, we performed a series of control experiments: First, we confirmed that PLGA-1NMPP1 microspheres effectively inhibit TrkA signaling in cultured sympathetic neurons obtained from $TrkA^{F592A}$ mice but not wild-type mice (Figure S6 E, I). Second, successful spatial inhibition of TrkA kinase activity and minimal effects from drug diffusion was confirmed in experiments that showed a dramatic loss of P-TrkA (Y785) puncta in neurons only within the injected ganglia, not in neurons of contralateral ganglia, of $TrkA^{F592A}$ mice (Figure 6B, C), and no obvious differences in P-TrkA (Y785) levels in TH positive axons innervating the ipsilateral iris (Figure 6D). Third, we confirmed pharmacogenetic specificity of the approach by observing no inhibition of P-TrkA signaling

in wild-type mice injected with PLGA-1NMPP1 microspheres or in *TrkA*^{F592A} mice injected with control microspheres (Figures 6C, S5A). Thus, 1NMPP1 loaded PLGA microspheres injected into the SCG enables specific inhibition of TrkA kinase activity exclusively within proximal axons, cell bodies and dendrites of sympathetic neurons of the injected ganglion and not within distal axons or neighboring tissues.

Remarkably, inhibition of somatodendritic TrkA kinase activity for only 6–8 hours resulted in a marked reduction in the number of post-synaptic Homer1 puncta and pre-synaptic VAChT puncta in injected ganglia as compared to uninjected, contralateral ganglia (Figures 6E–F, S5B). Importantly, this reduction was observed only in *TrkA*^{F592A} mice, not in wild-type mice, injected with 1NMPP1 loaded microspheres (Figures 6E–F, S5B). We next asked whether the decrease in SCG synapses following TrkA kinase inhibition in the somatodendritic compartment *in vivo* was associated with a corresponding functional disruption of SNS function. For this, we examined the eye region of treated animals because interruption of SNS circuitry results in ptosis, or eyelid droop, a symptom observed in patients with Horner's syndrome (Fields and Barker, 1992). Strikingly, ptosis was observed in the ipsilateral, but not contralateral eye of *TrkA*^{F592A} animals injected with 1NMPP1 loaded PLGA microspheres. This phenotype was not observed in mice injected with control microspheres or in wild-type mice receiving PLGA-1NMPP1 microspheres (Figures 6H–I, S5I). These experiments demonstrate that local TrkA endosome signaling, within the somatodendritic compartment of sympathetic neurons, is necessary for the proper number of synaptic complexes associated with dendrites as well as for SNS function *in vivo.*

Local TrkA kinase activity within dendrites is required for PSD maintenance

Our findings revealed a requirement of retrograde NGF-TrkA signaling within cell bodies, dendrites, or both, for synapse maintenance *in vivo.* The presence of signaling competent TrkA endosomes in dendrites and their close proximity to synapses *in vivo* and PSDs *in vitro* support the notion that TrkA endosome signaling within dendrites themselves promotes synapse maintenance. To distinguish between a requirement for TrkA endosome signaling in cell bodies or dendrites for synapse maintenance, we devised an experiment in which the effect of TrkA kinase activity inhibition solely within dendrites can be assessed. We adapted the use of 1NMPP1 loaded PLGA microspheres for *in vitro* microfluidic, compartmentalized sympathetic neuron experiments. To first test their efficacy, a large number of 1NMPP1-PLGA microspheres were applied exclusively to the somatodendritic compartment of cultured *TrkA*^{F592A} sympathetic neurons, thereby attaining sustained TrkA kinase inhibition within this compartment while simultaneously applying NGF exclusively to the distal axon compartment. PLGA-1NMPP1 microspheres, but not control PLGA microspheres, eliminated P-TrkA (Y785) puncta observed in cell bodies and dendrites of *TrkA*^{F592A} sympathetic neurons (Figure S6E, G). Importantly, P-TrkA immunoreactivity, and thus TrkA signaling, was observed at normal levels in distal axons, indicating the spatial specificity of this approach (Figure S6D).

To achieve selective inhibition within dendritic locales, a limiting number of biotinylated PLGA-1NMPP1 microspheres was applied to the somatodendritic compartment of neurons grown on streptavidin-coated coverslips, thus anchoring the microspheres and ensuring

release of 1NMPP1 in the same locations for the duration of the experiment (Figure 7A, B). Biotinylation did not alter the effectiveness of 1NMPP1-PLGA microspheres on TrkA^{F592A} kinase inhibition (Figure S6F). After 6–8 hours of biotinylated PLGA-1NMPP1 microsphere application, we measured the distance between the center of manually identified microspheres and fluorescent puncta above a specified intensity within dendrites. These experiments revealed a greater than two-fold increase in the distance between the locations of PLGA-1NMPP1 microspheres and P-TrkA puncta compared to that of control PLGA microspheres and P-TrkA puncta (Figure 7C, E), indicating effective, local inhibition of TrkA kinase activities within small regions of dendrites. Importantly, the number of P-TrkA puncta within neuronal cell bodies in control and PLGA-1NMPP1 microsphere conditions was not significantly different (Figure 7D, G). We also ensured that these results were not skewed by a difference in the distance between the microspheres and dendrites in the control and drug conditions (Figure 7F, I).

Having shown that PLGA-1NMPP1 microspheres could be used as a platform of sustained, focal 1NMPP1 release to create small pockets of local TrkA kinase inhibition, we next asked whether TrkA kinase signaling in dendrites, the soma, or both, is required to maintain post-synaptic density clusters. If P-TrkA signaling is necessary within dendrites to maintain PSDs, we would expect to find a decrease of MAGUK clusters in areas of TrkA kinase inhibition. Indeed, we found a significant increase in the distance from 1NMPP1 microspheres to the nearest MAGUK puncta within dendrites, compared to dendrites of neurons exposed to control microspheres (Figure 7 C, H). Taken together, these findings indicate that distal axon-derived TrkA endosome signaling within dendrites is necessary for maintenance of post-synaptic density clusters.

Discussion

How synaptic connections are formed and maintained is a central question in neuroscience. Here, a live cell imaging assay was used to reveal that TrkA endosome trafficking in sympathetic neuron axons, cell bodies and dendrites is remarkably distinct with respect to kinetics of movement and directionality. Moreover, signaling competent TrkA endosomes are often found within close proximity to synapses of sympathetic neuron dendrites *in vitro* as well as sympathetic neuron dendrites *in vivo*, throughout development. A chemical-genetic approach to locally inhibit TrkA kinase activity within the SCG *in vivo* was used to reveal the necessity of somatodendritic TrkA signaling for maintenance of both post-synaptic and pre-synaptic structures. The loss of somatodendritic TrkA signaling and synapses leads to ptosis, indicative of a deficit in SNS function. Importantly, spatially-restricted chemical-genetic inhibition of TrkA signaling within dendrites *in vitro* showed that TrkA endosome signaling within sympathetic neuron dendrites supports the maintenance of PSD clusters. Together, our findings show that peripheral target fields govern synaptic connectivity between preganglionic and postganglionic sympathetic neurons through distal axon-derived TrkA endosomes that traffic the entire length of postganglionic sympathetic neurons to signal locally, within their dendrites, to promote and maintain synapses (Figure S7).

TrkA endosome dynamics reflect function

We observed that TrkA endosomes in axons, cell bodies and dendrites move in a markedly different manner. In agreement with quantum dot-NGF tracking studies in sensory neurons (Cui et al., 2007), we found that TrkA endosomes within sympathetic neuron axons move solely retrogradely and in a saltatory manner with highly variable rates and intermittent pauses. Within axons, NGF endosomes are actively transported along uniformly oriented microtubules (Maday et al., 2014) by the motor protein dynein (Heerssen et al., 2004). In contrast to movement dynamics observed in axons, we found bidirectional movement of distal-axon derived TrkA endosomes within dendrites. Presuming the motor protein dynein underlies dendritic endosome trafficking, the bidirectionality of TrkA endosomes within dendrites may be explained by the mixed polarity of microtubules within that cellular compartment (Baas et al., 1991; Yau et al., 2016). Thus, we speculate that the distinct movement dynamics of TrkA endosomes within different cellular compartments reflects differences in cytoskeletal organization and dynein-microtubule interactions. Also, in contrast to axonal endosomal movement, TrkA endosomes in dendrites exhibit frequent oscillatory pauses in relatively small areas of the dendrite. Examination of mitochondrial motility has revealed similar findings; mitochondria in dendrites have a smaller excursion length than those in axons, which may be reflective of higher metabolic demands within dendrites (Li et al., 2004; Overly et al., 1996). It is likely that TrkA endosome dynamics also reflect functional requirements within different regions of the cell; the unidirectional and processive movement of TrkA endosomes in axons may reflect the necessity of retrograde transport to cell bodies to support somatic signaling, gene expression and survival, while the movement of TrkA endosomes in dendrites may reflect their function in that compartment for promoting and maintaining clustering of PSD proteins at synapses.

An interesting observation is that a substantial number of dendritically localized TrkA endosomes (~25%) are stationary. These endosomes may be targeted for degradation, and, consistent with this, stationary mitochondria in neuronal processes are thought to be targeted for proteasomal degradation upon disengagement from motor complexes (Wang et al., 2011). Stationary dendritic TrkA endosomes may thus be destined for degradation. Alternatively, stationary TrkA puncta in dendrites may reflect receptors that have been re-inserted or anchored to the plasma membrane (KML and DDG, unpublished); some of these are phospho-TrkA positive, which suggests they could act as signaling platforms to recruit PSD proteins. Further work addressing how the signaling state of TrkA endosomes affects their metabolism and dynamics may clarify this issue and provide insight into how TrkA endosome movement within dendrites corresponds to function. Noting that the maintenance of retrograde transport of NGF-containing endosomes in axons is independent of TrkA kinase activity (Ye et al., 2003), it will be interesting in the future to determine whether non-phosphorylated TrkA endosomes in dendrites are halted or return to the soma, and whether re-phosphorylation results in active movement or targeted transportation to dendrites. The present work indicates that endosomes of the same origin move differently depending on their cellular location, which likely reflects distinct states of TrkA activity and distinct functions within different regions of the neuron.

Long-distance endosome transport and signaling in dendrites may provide a general mechanism of circuit regulation

Our findings reveal a mechanism of neural circuit modification: target fields supply NGF to distal axons, initiating the formation of TrkA endosomes that are trafficked from axons into the cell body, and a subset move into dendrites where they signal locally to promote formation and maintenance of PSD clusters. NGF/TrkA signaling promotes PSD clustering in sympathetic neurons in a manner that is both independent of transcription (Sharma et al., 2010) and remarkably rapid (within three hours); however, the precise signals emanating from TrkA endosomes to support PSD formation remains to be elucidated. We observed that TrkA endosomes in dendrites are likely to signal through multiple downstream effector pathways; dendritic TrkA endosomes contain phosphorylated TrkA tyrosine residues 785 and 490, which associate with distinct sets of effectors and thus diversify the nature of the signal emanating from dendritic TrkA endosomes. It is noteworthy that our *in vivo* experiments that analyzed retrogradely trafficked WGA vesicles point to the presence of non-TrkA positive distal axon-derived vesicles. We speculate that these may contain additional signals that instruct sympathetic neuron development, dendritic growth and synaptic connectivity. Members of the BMP family are candidates for these processes, as they appear to contribute to sympathetic neuron dendrite length and complexity during developmental and adult periods (Majdazari et al., 2013). Thus, in addition to NGF, local signaling by other target-derived cues within dendrites may provide a general mechanism by which target fields instruct dendrite and synapse development and maintenance throughout the nervous system.

Local TrkA signaling, within dendrites, is necessary for synapse maintenance and function

Building on research implicating target-derived NGF in sympathetic neuron axon growth and target field innervation, survival, and synapse formation, the present work reveals a mechanism by which peripheral target fields regulate synaptic connectivity within the SNS. We found that the number of P-TrkA puncta within dendrites is correlated with the number of synapses during development. Moreover, using a spatially restricted and specific TrkA inhibition paradigm, we found that TrkA signaling within the SCG is essential for both presynaptic and postsynaptic specializations. In addition, blocking TrkA signaling within the SCG, thereby disrupting synapses, has readily apparent consequences—ptosis, a hallmark symptom of the SNS disorder Horner’s syndrome. Remarkably, both the decrease in synapse number and the ptosis phenotype resulting from TrkA inhibition within the ganglion were observed within 6–8 hours, emphasizing the importance of continual TrkA signaling in the somatodendritic compartment for SNS circuit function. These findings indicate that NGF-TrkA signaling is required *in vivo*, in the SCG itself, for proper functioning of postganglionic sympathetic neurons. This, together with the *in vitro* findings indicating a requirement of TrkA signaling within dendrites for PSD maintenance, supports a model whereby target field regulation of TrkA signaling within dendrites controls synapse development and maintenance, and possibly plasticity, thereby ensuring the proper function of SNS circuits.

This type of synaptic regulation controlled by target fields of sympathetic neurons may be at play in other neural circuits. Cholinergic neurons of the basal forebrain, for example, rely on

target-derived NGF signaling for maintenance of their biochemical and anatomical phenotype (Cuello et al., 2010; Parikh et al., 2013), and knockdown of TrkA expression results in Alzheimer's disease (AD) like symptoms in aged mice (Parikh et al., 2013; Sanchez-Ortiz et al., 2012). Investigating synapses that form upon forebrain cholinergic neurons may yield insight into the role retrograde NGF-TrkA signaling plays in preserving cholinergic neuron circuit function. As cholinergic neuron dysfunction in the CNS is implicated in ageing disorders such as AD as well as developmental disorders such as Down's syndrome (Schliebs and Arendt, 2011), how synapses of cholinergic forebrain neurons are formed and maintained by target fields may prove an important area of future research. Furthermore, many autism spectrum disorder and schizophrenia etiologies involve disruption of synapses, and more specifically, aberrant PSD proteins within developing circuits (de Bartolomeis et al., 2014). Thus, an exciting direction will be to determine the role of local dendritic signaling, orchestrated by trophic cues derived from target fields, in synapse development and maintenance within CNS circuits under both normal and disease states.

Experimental Procedures

Animal Studies

Mice were handled and housed in accordance with Harvard Medical School and Johns Hopkins University IACUC guidelines.

Compartmentalized Sympathetic Neuron Experiments

Dissociated SCG neurons were prepared (Wickramasinghe et al., 2008; Ye et al., 2003) and grown in microfluidic chambers as described (Park et al., 2006). The fixed cell Flag-TrkA transport assay was performed as described previously (Sharma et al., 2010). The live cell Flag-TrkA trafficking imaging assay used the Flag antibody (either M1 (1μg/mL) or FlagM1-FAB (6μg/mL)) incubated with 2μg/mL Alex Fluor secondary antibody, diluted in DMEM, for 1 hour at room temperature on a shaker, prior to application to distal axons and imaging. Imaging was done using a Yokogawa spinning disk microscope (Zeiss) or the Harvard Neurodiscovery Center Enhanced Neuroimaging Core Andor Revolution Spinning Disk Microscope, using fast piezo Z sectioning (Prior Piezo Stage with 250um travel - Z250). Trafficking analysis was done by manual tracking of individual endosomes using either IMARIS spot tracking or an ImageJ MTrackJ plugin (Meijering et al., 2012).

Eye Injections

Eye injections for retrograde labeling experiments were done using male mice (P21) anesthetized via continuous inhalation of isoflurane (1–3%) from a precision vaporizer for the 10 minute duration of the surgery. Sixteen hours following surgery animals were euthanized, SCGs were removed and standard IHC procedures were followed.

1NMPP1 PLGA Microsphere Experiments

Control (Phosphorex; PLGA 50:50, 5μm diameter) and 1NMPP1 loaded microspheres (Phosphorex; PLGA 50:50, 11.5% 1NMPP1 loading, 3μm diameter) were biotinylated, and applied to cell body and dendrite compartments of sympathetic neurons grown on coverslips

plated with streptavidin. After 1 hour, cultures were washed with DMEM to remove unbound microspheres. NGF was then applied to distal axons and cultures were incubated at 37°C for the duration of the experiment, 6–8 hours. Cultures were then fixed and used for ICC using standard procedures. For *in vivo* SCG injections of PLGA-1NMPP1 microspheres, a Hamilton syringe was used to inject 1–5μL of 0.5 mg microspheres diluted in 10 mL of 0.9% saline: either control (Phosphorex; PLGA 50:50, 5μm diameter) or 1NMPP1 loaded PLGA microspheres (Phosphorex; PLGA 50:50, 11.5% 1NMPP1 loading, 3μm diameter) were injected. Six-eight hours following surgery animals were sacrificed and SCGs were removed and processed for IHC.

Statistical Analysis

Statistical analysis was done using GraphPad Prism 6 software. Comparisons between two groups were done using Student's t test unless otherwise reported. Non-significant p values are not reported. Data are presented as mean ± SEM and numbers per group are represented in bars or legends of each panel.

Extended Experimental Procedures

Mouse lines, husbandry and genotyping

TrkA$^{F592A/F592A}$ mice (Chen et al., 2005) were maintained homozygous on a C57BL/6 background. The *TrkA*$^{F592A/F592A}$ mice are hypomorphic and exhibit lower levels of TrkA compared to wild-type mice (data not shown), explaining the fewer number of P-TrkA puncta observed in sympathetic neurons of *TrkA*$^{F592A/F592A}$ mice compared to wild-type mice. *TrkA*$^{Flag/Flag}$ mice (Sharma et al., 2010) were maintained homozygous on a mixed background. *TH*$^{-2A\text{-}CreER}$ (Abraira et al., 2017) heterozygous males were crossed to homozygous *Rosa*$^{-CAG\text{-}LSL\text{-}EYFP\text{-}WPRE}$ (Madisen et al., 2010) reporter mice and were genotyped for *TH-2A-CreER* using the following primer set which detect both mutant and wild- type alleles; TH-2A-CreER-1: CATGCCCATATCCAATCTCC, TH-2A-CreER-2: CTGGAGCGCATGCAGTAGTA, and TH-2A-CreER-3: ATGTTTAGCTGGCCCAAATG. Male and female mice were used for *in vitro* experiments and male mice were used for *in vivo* experiments. Analyses of wild-type neurons or tissue were performed on C57BL/6 or CD1 background mice. Mice were handled and housed in accordance with Harvard Medical School and Johns Hopkins University IACUC guidelines.

Sympathetic neuron cultures

SCG neurons were cultured as previously described (Wickramasinghe et al., 2008; Ye et al., 2003). In brief, neurons were obtained by enzymatic dissociation of P0–P4 mouse SCG, plated in DMEM supplemented with 10% fetal bovine serum (FBS), penicillin/streptomycin (1 U/ml), and 50 ng/ml NGF purified from mouse salivary glands or purchased (NGF 2.5S) from Harlan laboratories. After 24–48 hrs, 5 μM Ara-C was added to the culture media for 48–96 hrs to eliminate glial contamination. This resulted in long-term neuronal cultures that remained essentially glia-free for the duration of all experiments. Media was changed every 48 hrs, and all experiments commenced 14–16 DIV for mass cultures and microfluidic chambers (unless otherwise noted). SCG neurons were cultured in microfluidic chambers as previously described (Harrington et al., 2011; Sharma et al., 2010). In local TrkA inhibition

experiments using biotinylated PLGA microspheres, coverslips were coated with 5 μg/mL Streptavidin for 1 hour and rinsed twice with ddH_2O prior to plating of neurons.

Immunocytochemistry

Neurons were fixed in 4% PFA/1xPBS for 15 minutes at room temperature. After fixation, they were thoroughly washed in 1xPBS, blocked for 30–60 min in 5% Normal Goat Serum with 0.05% Triton-X in 1xPBS at room temperature, and incubated overnight at 4°C in 1% Normal Goat Serum block solution containing primary antibodies. Neurons were then rinsed in PBS, incubated with appropriate Alexa Flour fluorescent secondary antibodies in 5% Normal Goat Serum block solution for 60 min at room temperature, rinsed again in PBS, and subsequently mounted for confocal microscopy. Primary antibodies include pan-MAGUK K28/86 (1:500, Neuromab/Antibodies Inc.), MAP-2 (1:5000, Millipore 06-574), P-TrkA (Y785) (1:1000, Cell Signaling 4168S), P-TrkA (Y490) (1:1500, Cell Signaling 4691S), Flag-M1 (1:1000, Sigma-Aldrich F3040), Flag (1:1000 Sigma-Aldrich F7425), Homer1 (1:1000 Synaptic Systems 160003).

Microfluidic chambers

Microfluidic chambers were generated as previously described (Park et al., 2006). Masks were designed in AutoCad and made by Photo Sciences Inc. Molds were generated in the Johns Hopkins Whitaker Institute Lithography and Fabrication Facility.

Flag-TrkA transport assay

Assay was performed as described previously (Sharma et al., 2010). Cells were NGF starved overnight at 37°C in DMEM. The following day, cells were habituated to 4°C for 10–15 minutes, then Flag antibody, either M1 (1 μg/mL) or FlagM1-FAB (6 μg/mL) diluted in DMEM was applied to only the distal axon compartment at 4°C for 45 min- 1 hour. Cells were washed in DMEM to remove any unbound antibody, then NGF (50–100 μg/mL) diluted in DMEM was applied only to the distal axon compartment. Complete compartmentalization of both antibody and ligand to the distal axons was achieved using microfluidic chambers, with a volume of 80 μL added to distal axon compartment and a volume of 120 μL added to cell body/dendrite compartment. After NGF application cells were incubated in a humidified 10% CO2 incubator at 37°C for 1–6 hours depending on the purpose of the experiment. Cells were then immunostained according to *in vitro* immunostaining protocol above.

Live cell imaging Flag-TrkA assay

The live cell Flag-TrkA trafficking assay was completed the same as the fixed Flag-TrkA assay with one exception: Flag antibody, either M1 (1 μg/mL) or FlagM1-FAB (6 μg/mL) was incubated with 2 μg/mL Alexa Fluor secondary antibody, diluted in DMEM, for 1 hour at room temperature on a shaker, prior to application to distal axons. To image Flag- TrkA endosomes' dynamics in real time without harming neuronal health, three conditions must be met: there must be proper CO_2 buffering, the temperature must remain consistently 36–37°C, and the chambers must stay hydrated. The first was achieved either by using a CO2-independent ACSF medium (120mM NaCl, 5mM KCl, 5mM $CaCl_2$, 2mM $MgCl_2$, 25mM

HEPES (pH 7.4), 30mM glucose) or a CO_2 buffered chamber on the spinning disk microscope. Temperature was maintained through feedback monitors linked to the microscope stage. Hydration was maintained either through adding new ACSF media or via humidified stages on the microscope. Imaging was achieved in the following manner: the glass coverslip, with microfluidic chamber attached, was removed from the petri dish and placed onto the microscope stage, where it was be imaged using either 40xO (NA: 1.30) or 60xO (NA: 1.42) magnification objectives. Imaging was completed on a Yokogawa spinning disk microscope (Zeiss) or the Harvard Neurodiscovery Center Enhanced Neuroimaging Core Andor Revolution Spinning Disk Microscope, using fast piezo Z sectioning (Prior Piezo Stage with 250um travel - Z250). The latter microscope achieved temperature, CO_2, and humidity maintenance by both a whole scope incubator and small stage top incubator. Videos were taken with maximum speed acquisition allowed by the number of 1μm Z slices necessary to capture the depth of the dendrite and cell body of interest. Photobleaching was achieved by applying maximum 488 laser intensity to the cell of interest for 5 minutes. At the end of the live cell experiments, cells were fixed and immunostained according to *in vitro* immunostaining protocol above and mounted for confocal microscopy.

Tissue immunohistochemistry

SCG sections were produced by dissecting the ganglia from mice euthanized via CO_2 and fixing the ganglia in 4% PFA/1xPBS at room temperature for one hour. Fixed and washed tissue was cryoprotected in 30% sucrose, embedded in OCT, and cryosectioned at a thickness of 20μm. For WGA-555 eye injection experiments, sections were rehydrated in 1xPBS, blocked for 30–60 min (5% Normal Goat Serum, 0.05% Triton-X in 1xPBS), and incubated in primary antibody diluted in block overnight at 4°C. They were subsequently washed in 1xPBS, incubated with appropriate Alexa Fluor fluorescent secondary antibodies for 60 min at room temperature, washed in PBS, and then mounted for confocal microscopy. For all other experiments, an alternative, high salt protocol was used. For this, cryosections were rehydrated in 1xPBS, incubated in 50% EtOH for 30 min, then washed in high salt PBS (0.3M NaCl) and incubated in appropriate primary antibodies diluted in high salt PBST (0.3M NaCl, 0.03% Triton-X) for 48–72 hours at 4°C. Sections were subsequently washed in high salt PBS, incubated with appropriate Alexa Fluor fluorescent secondary antibodies for 60 min at room temperature, washed in high salt PBS, and then mounted for confocal microscopy. Primary antibodies include TrkA (1:1000, Millipore 06-574), P-TrkA (Y785) (1:1000, Cell Signaling 4168S), Flag-M1 (1:1000, Sigma F7425), Homer1 (1:1000, Synaptic Systems 160003), MAP2 (1:2500, Millipore AB5543), GFP (1:1000, Aves GFP 1020), and VAChT (1:200, Enzo Life Sciences BML-SA684-0100).

Intraperitoneal injections for P-TrkA antibody specificity measurements

To address the specificity of P-TrkA antibodies *in vivo*, the inhibitor 1NMPP1 was dissolved in DMSO to make a 200mM stock, and 2.5 μL of the 1NMPP1 solution or DMSO was diluted into 100 μL of injection solution (0.9% NaCl, 2.5% Tween-20) for intraperitoneal injections. Treatments were given every hour for a total of four times, in P10–P12 aged $TrkA^{F592A/F592A}$ mice. 1NMPP1 was synthesized by Aurora Analytics LLC.

Retrograde eye injections

10 μL WGA-555 was injected into the anterior chamber of the eye of anesthetized P21–P30 male mice using a Hamilton syringe as previously described (Hendry et al., 1974). Mice were euthanized 16–20 hours later via CO_2. SCGs were dissected out and standard immunohistochemical tissue processing procedures (above) were followed.

Tamoxifen treatment

One week before sacrifice and dissection of superior cervical ganglia, tamoxifen was administered to the mice at a dose that would achieve sparse labeling of neurons. (0.005 mg for P7, 0.01mg P14 and P21, and 0.1mg postnatal 6–8 wks) Tamoxifen was dissolved in ethanol (20 mg/ml), mixed with equal volume of sunflower seed oil (Sigma), vortexed for 5–10 mins and centrifuged under vacuum for 20–30 mins to remove all ethanol. The solution was kept at −20°C and delivered via IP injection. SCGs were dissected at P7, P14, P21, and postnatal 6–8 weeks.

SCG microsphere injections

Male mice (P21) were anesthetized via continuous inhalation of isoflurane (1–3%) from a precision vaporizer for the 20 minute duration of the surgery. Breathing rate of each animal was monitored throughout the procedure, with adjustments to anesthetic dose made as necessary. Puralube, a protective eye ointment, was applied to the eyes while they were in the nose cone. To inject SCGs with microspheres, the area of the ipsilateral SCG was treated with depilatory cream (NAIR, Church and Dwight Co.), for 1 min, washed with water, and then swabbed with 70% Ethanol and Betadine before incision. An incision was made to the front of the neck, lateral to the midline. Fat, muscle, and glands were cut or moved aside to expose the SCG, residing at the juncture of the internal and external carotoid arteries. Next, a Hamilton syringe was used to puncture the membrane of the SCG and inject 1–5uL of 0.5 mg microspheres diluted in 10 mLs of 0.9% saline: either control (Phosphorex; PLGA 50:50, 5μm diameter) or 1NMPP1 loaded PLGA microspheres (Phosphorex; PLGA 50:50, 11.5% 1NMPP1 loading, 3μm diameter) were used. Skin was sutured using sterile vicryl sutures, then swabbed with NewSkin adhesive (Fisher). Carprofen (4 mg/kg) was applied subcutaneously for analgesia immediately following the procedure, and animals recovered in isolation on a heating pad for 30 minutes. Six- eight hours following surgery animals were euthanized, their SCGs were dissected out and standard immunohistochemical tissue processing procedures (above) were followed.

In vitro PLGA microsphere assays

PLGA microspheres were biotinylated to anchor them to streptavidin coated coverslips for *in vitro* local TrkA kinase inhibition experiments. Both control (Phosphorex; PLGA 50:50, 5μm diameter) and 1NMPP1 loaded microspheres (Phosphorex; PLGA 50:50, 11.5% 1NMPP1 loading, 3μm diameter) were biotinylated according to the following protocol. 0.5 mg microspheres were diluted in 1 mL of MES buffer (0.1mM MES pH5.5) then incubated with 140 μL of 50mM Amine-PEG-Biotin (Thermo-Scientific Pierce) in MES buffer solution and 60 μL 100 mM EDC (Thermo-Scientific Pierce) in MES buffer solution for 1 hour on a shaker at room temperature. Solution was dialyzed using Pierce Slide-A-Lyzer

20,000 MWCO dialysis cassettes in MES buffer at 4°C for 30 minutes. Dialyzed microsphere solution was added to DMEM to bring to 10 mL solution and pH was brought to 7.4. This solution was further diluted 1:50 unless otherwise specified into DMEM and applied to the cell body and dendrite compartment of sympathetic neurons grown on coverslips plated with streptavidin. After 1 hour for biotin-streptavidin binding cultures were washed with DMEM to remove any unbound microspheres. NGF was applied to the distal axon and cultures were incubated at 37°C for the duration of the experiment, 6–8 hours. Cultures were then fixed and immunostained as described above.

Image Analysis

Endosome tracking—Image analysis was completed through manual tracking of individual endosomes either using IMARIS spot tracking or the ImageJ MTrackJ plugin written by Erik Meijering (Meijering et al., 2012). Directionality was defined as moving in a direction for 2 or more sequential image frames. Post-hoc MAP2 staining or DIC imaging was used to verify dendrites. Kymographs were made in ImageJ using the Reslice and projection (StDev) functions.

In vitro proximity of P-TrkA and MAGUK—Dendrites stained for P-TrkA, MAGUK, and MAP2 were imaged on an LSM700 Zeiss Confocal Microscope using a 63x objective acquiring images that had 0.05μm sized pixels. Proximity was analyzed using a MATLAB script written by the Harvard Image Data Analysis Core. Specifically, manual thresholding of MAP2 stained dendrites was performed to identify areas of interest. Robust point source detection and Gaussian PSF-model fitting were then performed within each dendrite area to identify both MAGUK and P-TrkA puncta with a precision ranging from approximately 15–70nm (Aguet et al., 2013). A distance-based co-localization measure was then calculated as previously described (Lachmanovich et al., 2003; Mendoza et al., 2011). Briefly, closest distances between points in the two image channels (MAGUK and P-TrkA) were calculated, and a frequency vs. search radius curve generated. This curve was then normalized to the mean frequency of interpoint distances observed in 500 rounds of randomly generated point positions with the same number of points and within the same dendrite area. These 500 rounds of randomization were conducted in two ways: once holding points from image channel one (P-TrkA) fixed while randomizing channel two (MAGUK), and a second time holding points from image channel two while randomizing channel one. Performing randomizations in both channels controls for the fact that spatial patterns in the points in one channel can potentially induce unauthentic indications of co-localization in the other channel. No difference was seen between these alternate randomizations. Significance of co-localization within each dendrite was determined by comparing the measured density vs. distance to the 99^{th} percentile of the density seen in the 500 randomizations in that cell. For analysis combining multiple dendrites from multiple experiments, the normalized density curves for each cell were averaged and a 99% confidence interval was then calculated at each distance by 5000 bootstrap repetitions, by sampling from the individual dendrite curves with replacement. Significance was determined by comparing these confidence intervals to what would be expected purely by chance, represented as 1, which is the normalized frequency at any given distance. Nearest-neighbor distances were also calculated between

points to determine the fraction of points within the 100 nm cutoff from one another. The co-localization code is available upon request from the Image and Data Analysis Core at Harvard Medical School (http://idac.hms.harvard.edu/).

Puncta analysis—In experiments where numbers of puncta (P-TrkA, VACHT, Homer) were quantified, analysis was performed using ImageJ. Each channel of each image was thresholded, and the particle analysis function was used to summarize the number and size of puncta within the channel, which was further analyzed relative to area (μm^2), number of cell bodies, or dendrite length (μm). Co-localization analysis was completed also using ImageJ. Channel one and channel two were individually thresholded to binary images and the number of puncta within each channel was quantified using the Analyze Particles function. Next, the binary images were processed using the Image Calculator function to identify pixels/puncta that were fluorescent (1 in binary terms) in both channels, and the number and size of these “co-localized” puncta were quantified. For developmental analysis the number of puncta (P-TrkA, VACHT, Homer) were quantified using an ImageJ macro. To select the dendrite, a binary mask was created by manually thresholding the *TH-2A-CreER; R26-LSL-YFP* channel. The mask was despeckled and dilated. The other channels in the image were multiplied by the mask and thresholded with a set intensity to select puncta. The particle analysis function was used to summarize the number and size of puncta within each channel. Co-localization analysis was also completed using the ImageJ macro. The two channels were combined using the Image Calculator function and the particle analysis function was used to qualify the co-localized regions. Puncta numbers were divided by the area of the dendrite mask for each image. The area was calculated from the integrated density of the binary mask image.

In vivo nearest neighbor analysis—The nearest neighbor (VACHT) for each puncta (P-TrkA, Homer) was calculated using an ImageJ macro. The particle analysis function was used to summarize the centroid of the puncta within each channel of the thresholded and masked image. For each channel the xyz coordinates of each puncta were stored in an array. Within each z-slice, the distance between each puncta in one channel and all the puncta in the other channel was calculated. The shortest distance within 15μm was found, where both puncta were within the same dendrite mask region.

Measuring ptosis—Images for ptosis analysis were taken of animals anesthetized with urethane using infrared light sources and a Point Grey camera (FMVU-13S2C-CS) with a Navitar HR F2.8/50 mm lens borrowed from the Research Instrumentation Core Facility at HMS. Images were analyzed blinded by using ImageJ to draw and measure lines for the width and height of the eye surface then using a height/width ratio to compare amongst animals and groups.

Measurement distances between microspheres and fluorescent puncta—Data was analyzed using an ImageJ macro. After microspheres within each image were manually selected as regions of interest (ROIs) each image was processed through the program as follows: 1) cell bodies were chosen as ROIs to be eliminated from the analysis 2) each channel (P-TrkA, MAGUK, MAP2) was manually thresholded to identify objects of each

channel and the image was binarized 3) using the Image Calculator 'AND' function, MAP2 and both puncta channels were combined to identify puncta within dendrites 4) center of microsphere ROIs was identified 5) the program used an algorithm to measure the distance between identified puncta and each microsphere and created a spreadsheet with the results of the nearest distance (μm) as well as the size of the nearest identified puncta and the distance of microsphere ROI to dendrite.

Statistical Analysis

Statistical tests were performed using GraphPad Prism 6 software. Comparisons between two groups were done using Student's t test unless otherwise reported. Non-significant p values are not reported. Data are presented as mean ± SEM and numbers per group are represented in bars or legends of each panel.

Supplementary Material

Refer to Web version on PubMed Central for supplementary material.

Acknowledgments

We thank Clinton Cave, Chenghua Gu, Tracy Huang, David Paul and members of the Ginty lab for discussion and comments on the manuscript. We thank Amanda Zimmerman (HMS) for use of *TH-2A-CreER* mouse line. We thank Mollie Meffert for use of the Yokogawa spinning disc confocal microscope, Michele Pucak of the JHMI Multiphoton Imaging Core, Lai Ding and Daniel Tom of the Harvard NeuroDiscovery Center, and Michelle Ocana of the HMS Neurobiology Imaging Facility for microscope training and advice on imaging and analysis. We thank Hunter Elliott of the Harvard IDAC Core for image analysis advice and the close proximity script. We thank William Colgan (HMS) and Daniel Tom for creating ImageJ macros for puncta analysis and microsphere analysis, respectively. We thank the Harvard Research Instrumentation Core for equipment. We thank Huy Vo of the Johns Hopkins BME Machine Shop for microfluidic device advice and fabrication. This work was supported by NIH grant NS34814 (DDG) and an IES Brain Research Foundation Fellowship (KMW). DDG is an investigator of the Howard Hughes Medical Institute.

References

Abraira VE, Kuehn ED, Chirila AM, Springel MW, Toliver AA, Zimmerman AL, Orefice LL, Boyle KA, Bai L, Song BJ, et al. The Cellular and Synaptic Architecture of the Mechanosensory Dorsal Horn. Cell. 2017; 168:295–310.e219. [PubMed: 28041852]

Baas PW, Slaughter T, Brown A, Black MM. Microtubule dynamics in axons and dendrites. J Neurosci Res. 1991; 30:134–153. [PubMed: 1795398]

Barford K, Deppmann C, Winckler B. The neurotrophin receptor signaling endosome: where trafficking meets signaling. Dev Neurobiol. 2016

Campenot RB. Local control of neurite development by nerve growth factor. Proc Natl Acad Sci U S A. 1977; 74:4516–4519. [PubMed: 270699]

Chen X, Ye H, Kuruvilla R, Ramanan N, Scangos KW, Zhang C, Johnson NM, England PM, Shokat KM, Ginty DD. A chemical-genetic approach to studying neurotrophin signaling. Neuron. 2005; 46:13–21. [PubMed: 15820690]

Cuello AC, Bruno MA, Allard S, Leon W, Iulita MF. Cholinergic involvement in Alzheimer's disease. A link with NGF maturation and degradation. J Mol Neurosci. 2010; 40:230–235. [PubMed: 19680822]

Cui B, Wu C, Chen L, Ramirez A, Bearer EL, Li WP, Mobley WC, Chu S. One at a time, live tracking of NGF axonal transport using quantum dots. Proc Natl Acad Sci U S A. 2007; 104:13666–13671. [PubMed: 17698956]

de Bartolomeis A, Latte G, Tomasetti C, Iasevoli F. Glutamatergic postsynaptic density protein dysfunctions in synaptic plasticity and dendritic spines morphology: relevance to schizophrenia and

other behavioral disorders pathophysiology, and implications for novel therapeutic approaches. Mol Neurobiol. 2014; 49:484–511. [PubMed: 23999870]

Fields CR, Barker FM 2nd. Review of Horner's syndrome and a case report. Optom Vis Sci. 1992; 69:481–485. [PubMed: 1641232]

Glebova NO, Ginty DD. Heterogeneous requirement of NGF for sympathetic target innervation in vivo. J Neurosci. 2004; 24:743–751. [PubMed: 14736860]

Harrington AW, St Hillaire C, Zweifel LS, Glebova NO, Philippidou P, Halegoua S, Ginty DD. Recruitment of actin modifiers to TrkA endosomes governs retrograde NGF signaling and survival. Cell. 2011; 146:421–434. [PubMed: 21816277]

Heath JW, Glenfield PJ, Rostas JA. Structural maturation of synapses in the rat superior cervical ganglion continues beyond four weeks of age. Neurosci Lett. 1992; 142:17–21. [PubMed: 1407711]

Heerssen HM, Pazyra MF, Segal RA. Dynein motors transport activated Trks to promote survival of target-dependent neurons. Nat Neurosci. 2004; 7:596–604. [PubMed: 15122257]

Hendry IA, Stockel K, Thoenen H, Iversen LL. The retrograde axonal transport of nerve growth factor. Brain Res. 1974; 68:103–121. [PubMed: 4143411]

Heumann R, Korsching S, Scott J, Thoenen H. Relationship between levels of nerve growth factor (NGF) and its messenger RNA in sympathetic ganglia and peripheral target tissues. EMBO J. 1984; 3:3183–3189. [PubMed: 6549295]

Hu YB, Dammer EB, Ren RJ, Wang G. The endosomal-lysosomal system: from acidification and cargo sorting to neurodegeneration. Transl Neurodegener. 2015; 4:18. [PubMed: 26448863]

Huang S, O'Donovan KJ, Turner EE, Zhong J, Ginty DD. Extrinsic and intrinsic signals converge on the Runx1/CBFbeta transcription factor for nonpeptidergic nociceptor maturation. Elife. 2015; 4:e10874. [PubMed: 26418744]

Jiang X, Nardelli J. Cellular and molecular introduction to brain development. Neurobiol Dis. 2016; 92:3–17. [PubMed: 26184894]

Kuruvilla R, Ye H, Ginty DD. Spatially and functionally distinct roles of the PI3-K effector pathway during NGF signaling in sympathetic neurons. Neuron. 2000; 27:499–512. [PubMed: 11055433]

Kuruvilla R, Zweifel LS, Glebova NO, Lonze BE, Valdez G, Ye H, Ginty DD. A neurotrophin signaling cascade coordinates sympathetic neuron development through differential control of TrkA trafficking and retrograde signaling. Cell. 2004; 118:243–255. [PubMed: 15260993]

Levi-Montalcini R, Booker B. Destruction of the Sympathetic Ganglia in Mammals by an Antiserum to a Nerve-Growth Protein. Proc Natl Acad Sci U S A. 1960; 46:384–391. [PubMed: 16578497]

Li Z, Okamoto K, Hayashi Y, Sheng M. The importance of dendritic mitochondria in the morphogenesis and plasticity of spines and synapses. Cell. 2004; 119:873–887. [PubMed: 15607982]

Maday S, Twelvetrees AE, Moughamian AJ, Holzbaur EL. Axonal transport: cargo-specific mechanisms of motility and regulation. Neuron. 2014; 84:292–309. [PubMed: 25374356]

Majdazari A, Stubbusch J, Muller CM, Hennchen M, Weber M, Deng CX, Mishina Y, Schutz G, Deller T, Rohrer H. Dendrite complexity of sympathetic neurons is controlled during postnatal development by BMP signaling. J Neurosci. 2013; 33:15132–15144. [PubMed: 24048844]

Makadia HK, Siegel SJ. Poly Lactic-co-Glycolic Acid (PLGA) as Biodegradable Controlled Drug Delivery Carrier. Polymers (Basel). 2011; 3:1377–1397. [PubMed: 22577513]

Meijering E, Dzyubachyk O, Smal I. Methods for cell and particle tracking. Methods Enzymol. 2012; 504:183–200. [PubMed: 22264535]

Nja A, Purves D. The effects of nerve growth factor and its antiserum on synapses in the superior cervical ganglion of the guinea-pig. J Physiol. 1978; 277:53–75. [PubMed: 206691]

Overly CC, Rieff HI, Hollenbeck PJ. Organelle motility and metabolism in axons vs dendrites of cultured hippocampal neurons. J Cell Sci. 1996; 109(Pt 5):971–980. [PubMed: 8743944]

Parikh V, Howe WM, Welchko RM, Naughton SX, D'Amore DE, Han DH, Deo M, Turner DL, Sarter M. Diminished trkA receptor signaling reveals cholinergic-attentional vulnerability of aging. Eur J Neurosci. 2013; 37:278–293. [PubMed: 23228124]

Park JW, Vahidi B, Taylor AM, Rhee SW, Jeon NL. Microfluidic culture platform for neuroscience research. Nat Protoc. 2006; 1:2128–2136. [PubMed: 17487204]

Riccio A, Pierchala BA, Ciarallo CL, Ginty DD. An NGF-TrkA-mediated retrograde signal to transcription factor CREB in sympathetic neurons. Science. 1997; 277:1097–1100. [PubMed: 9262478]

Ruit KG, Osborne PA, Schmidt RE, Johnson EM Jr, Snider WD. Nerve growth factor regulates sympathetic ganglion cell morphology and survival in the adult mouse. J Neurosci. 1990; 10:2412–2419. [PubMed: 2376779]

Ruit KG, Snider WD. Administration or deprivation of nerve growth factor during development permanently alters neuronal geometry. J Comp Neurol. 1991; 314:106–113. [PubMed: 1797866]

Sanchez-Ortiz E, Yui D, Song D, Li Y, Rubenstein JL, Reichardt LF, Parada LF. TrkA gene ablation in basal forebrain results in dysfunction of the cholinergic circuitry. J Neurosci. 2012; 32:4065–4079. [PubMed: 22442072]

Schliebs R, Arendt T. The cholinergic system in aging and neuronal degeneration. Behav Brain Res. 2011; 221:555–563. [PubMed: 21145918]

Senger DL, Campenot RB. Rapid retrograde tyrosine phosphorylation of trkA and other proteins in rat sympathetic neurons in compartmented cultures. J Cell Biol. 1997; 138:411–421. [PubMed: 9230082]

Sharma N, Deppmann CD, Harrington AW, St Hillaire C, Chen ZY, Lee FS, Ginty DD. Long-distance control of synapse assembly by target-derived NGF. Neuron. 2010; 67:422–434. [PubMed: 20696380]

Smolen A, Raisman G. Synapse formation in the rat superior cervical ganglion during normal development and after neonatal deafferentation. Brain research. 1980; 181:315–323. [PubMed: 7350969]

Sofroniew MV, Howe CL, Mobley WC. Nerve growth factor signaling, neuroprotection, and neural repair. Annu Rev Neurosci. 2001; 24:1217–1281. [PubMed: 11520933]

Taylor AM, Dieterich DC, Ito HT, Kim SA, Schuman EM. Microfluidic local perfusion chambers for the visualization and manipulation of synapses. Neuron. 2010; 66:57–68. [PubMed: 20399729]

Tsui-Pierchala BA, Ginty DD. Characterization of an NGF-P-TrkA retrograde-signaling complex and age-dependent regulation of TrkA phosphorylation in sympathetic neurons. J Neurosci. 1999; 19:8207–8218. [PubMed: 10493722]

Voyvodic JT. Development and regulation of dendrites in the rat superior cervical ganglion. J Neurosci. 1987; 7:904–912. [PubMed: 3559715]

Wang X, Winter D, Ashrafi G, Schlehe J, Wong YL, Selkoe D, Rice S, Steen J, LaVoie MJ, Schwarz TL. PINK1 and Parkin target Miro for phosphorylation and degradation to arrest mitochondrial motility. Cell. 2011; 147:893–906. [PubMed: 22078885]

Watson FL, Heerssen HM, Moheban DB, Lin MZ, Sauvageot CM, Bhattacharyya A, Pomeroy SL, Segal RA. Rapid nuclear responses to target-derived neurotrophins require retrograde transport of ligand-receptor complex. J Neurosci. 1999; 19:7889–7900. [PubMed: 10479691]

Wickramasinghe SR, Alvania RS, Ramanan N, Wood JN, Mandai K, Ginty DD. Serum response factor mediates NGF-dependent target innervation by embryonic DRG sensory neurons. Neuron. 2008; 58:532–545. [PubMed: 18498735]

Yau KW, Schatzle P, Tortosa E, Pages S, Holtmaat A, Kapitein LC, Hoogenraad CC. Dendrites In Vitro and In Vivo Contain Microtubules of Opposite Polarity and Axon Formation Correlates with Uniform Plus-End-Out Microtubule Orientation. J Neurosci. 2016; 36:1071–1085. [PubMed: 26818498]

Ye H, Kuruvilla R, Zweifel LS, Ginty DD. Evidence in support of signaling endosome-based retrograde survival of sympathetic neurons. Neuron. 2003; 39:57–68. [PubMed: 12848932]

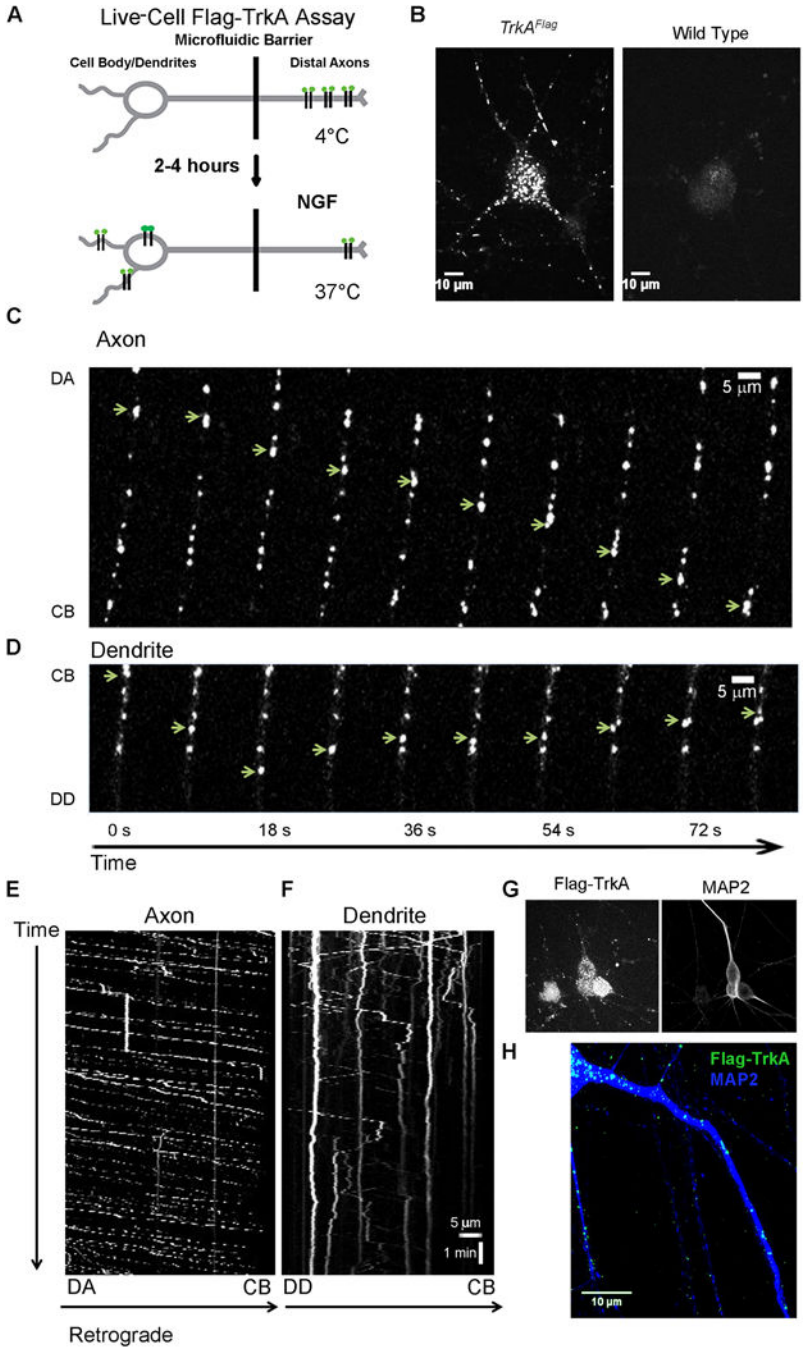

Figure 1. Live cell imaging reveals distinct trafficking dynamics of distal axon derived TrkA endosomes in different neuronal compartments

A. Schematic of the live cell Flag-TrkA endosome visualization assay to assess movement of TrkA endosomes in axons, soma and dendrites of sympathetic neurons. **B.** Live cell images of TrkA endosomes in *TrkA*^{Flag} neurons (left) and wild-type neurons (right). **C.** Individual Flag-TrkA endosomes in axons tracked in real time moving retrogradely from distal axons (DA) towards the cell body (CB). **D.** Individual Flag-TrkA endosomes in dendrites tracked in real time moving towards the distal dendrite (DD), some switching directions and moving

towards the CB. In C and D each image represents a frame acquired every 3.0 seconds. Arrows denote one endosome over time. **E.** Kymograph of Flag-TrkA endosome movement in axons from time lapse images acquired every 2.3 seconds. **F.** Kymograph of Flag-TrkA endosome movement in dendrites from same video in E. E and F spatial and temporal scale is the same. **G.** Live cell Flag-TrkA endosomes align with *post hoc* IHC for MAP2, a dendritic marker. **H.** Retrogradely trafficked TrkA endosomes are found throughout the MAP2+ dendritic arbor of sympathetic neurons. See also Figure S1.

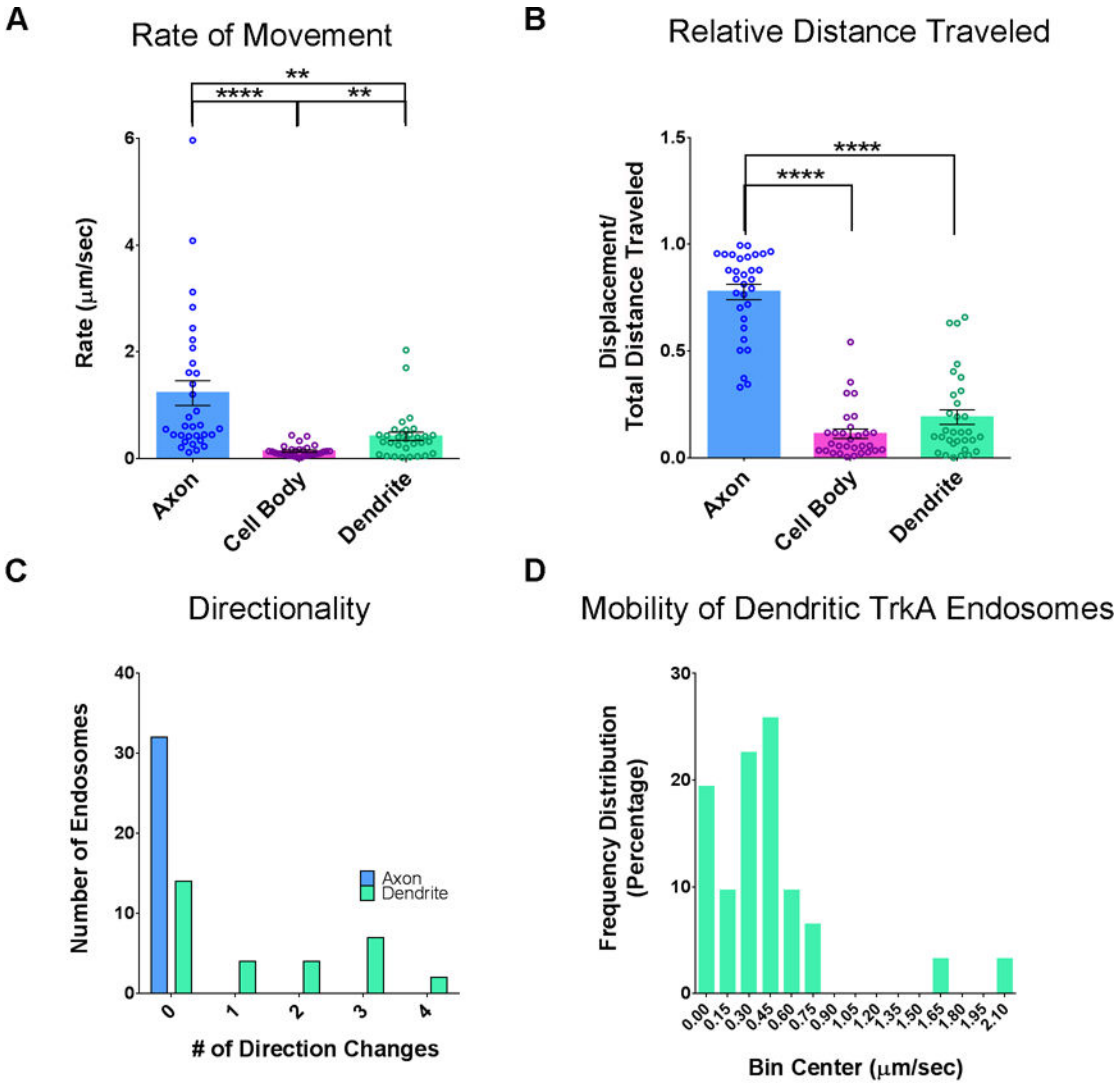

Figure 2. Comparison of TrkA endosome movement dynamics within different cellular compartments

A. The average rate of movement of Flag-TrkA endosomes tracked in axons, cell bodies and dendrites, including stationary endosomes. Kruskal-Wallis test P<0.0001 F (2, 90) = 41.00; *post hoc* Dunn's multiple comparisons' test: for axon vs cell body (CB): ****p<0.0001; for axon vs dendrite **p<0.001; for CB vs dendrite **p<0.001. **B.** Quantification of relative distance traveled by endosomes in each cellular compartment (displacement over total net movement). Kruskal-Wallis test P<0.0001 F (2, 89) = 57.72; *post hoc* Dunn's multiple comparisons' test: for axon vs CB: ****p<0.0001; for axon vs dendrite ****p<0.0001. A and B n(axon) = 32, n(CB) = 30, n(dendrite) = 31. **C.** Histogram denoting the number of times an individual endosome changes its direction. **D.** Frequency distribution of the rate (μm/sec) of TrkA endosomes within dendrites. The first bin is categorized as stationary. Bin size is 0.15 μm/sec. Data are presented as mean ± SEM. See also Figure S1.

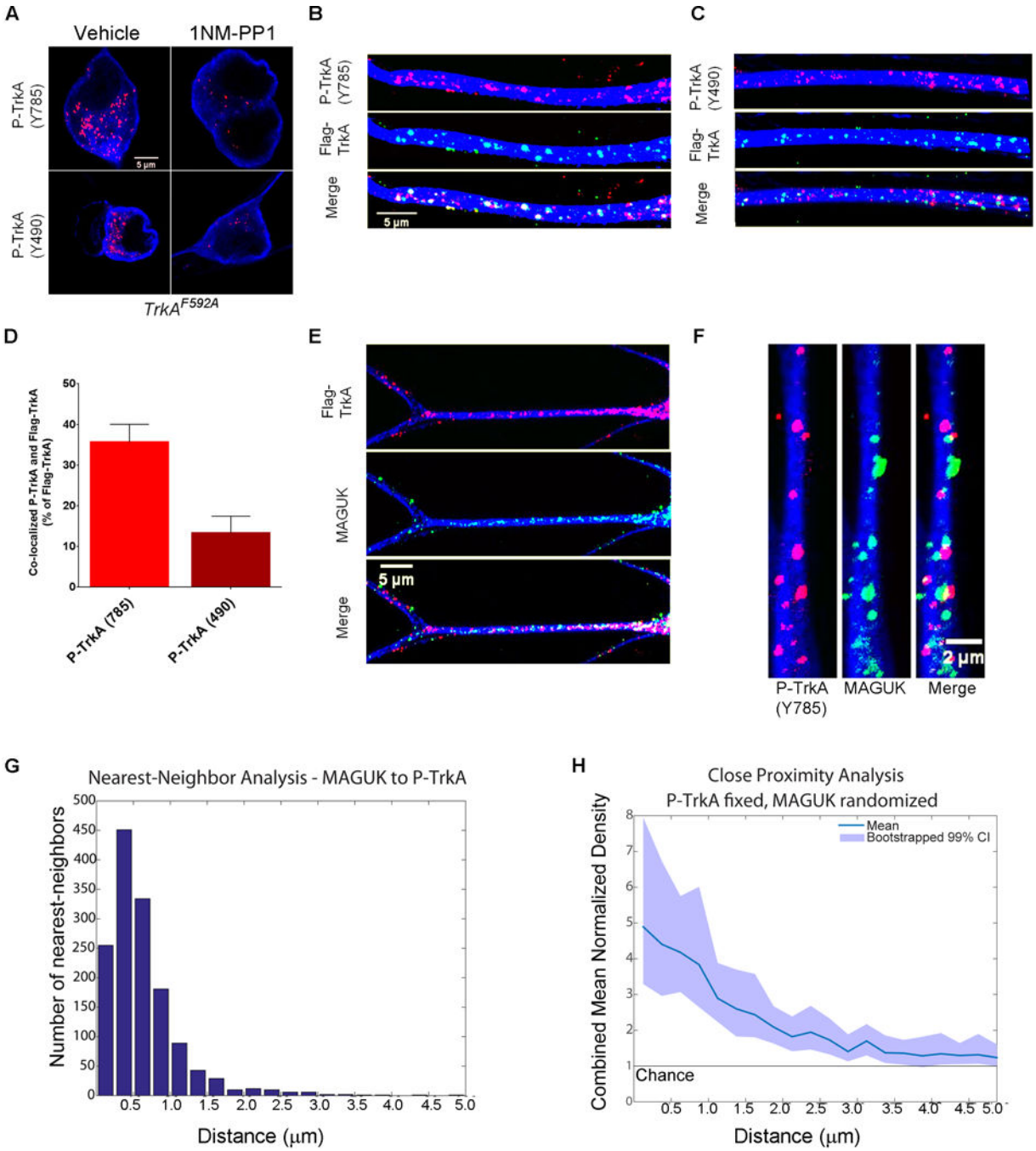

Figure 3. Distal axon-derived TrkA endosomes in dendrites are signaling competent and localized in close proximity to PSDs

A. Images of *TrkA*^{F592A} cell bodies immunostained for P-TrkA (Y785) puncta in both vehicle (top left) and 1NMPP1 (top right) conditions, as well as cell bodies immunostained for P-TrkA (Y490) puncta in both vehicle (bottom left) and 1NMPP1 (bottom right) conditions, showing specificity of P-TrkA antibodies. B–H represent data 3–6 hours after NGF application to the distal axon compartment. **B, C.** Images illustrating co-localization of retrograde Flag-TrkA endosomes and P-TrkA (Y785) (B) and Y490 (C) in dendrites. C is

same scale as B. **D.** Quantification of co-localization between retrogradely trafficked Flag-TrkA endosomes and P-TrkA (Y785) and P-TrkA (Y490) (n=3). **E.** Images of distal axon-derived Flag-TrkA endosomes (top) in close proximity to the PSD protein MAGUK (middle) in dendrites of sympathetic neurons. **F.** High magnification image of P-TrkA puncta (left) within dendrites in close proximity to MAGUK puncta (middle). **G.** Histogram of nearest neighbor analysis of nearest MAGUK puncta to P-TrkA (Y785) puncta. **H.** Population level analysis comparing the proximity of P-TrkA (Y785) and MAGUK puncta to that expected by chance, represented on the y-axis as 1. Transparent band shows 99% confidence intervals determined by bootstrapping. G,H n=22 dendrites, 4 chambers, 2 independent experiments. A–F MAP2 ICC is in blue. Data are presented as mean ± SEM. See also Figure S2.

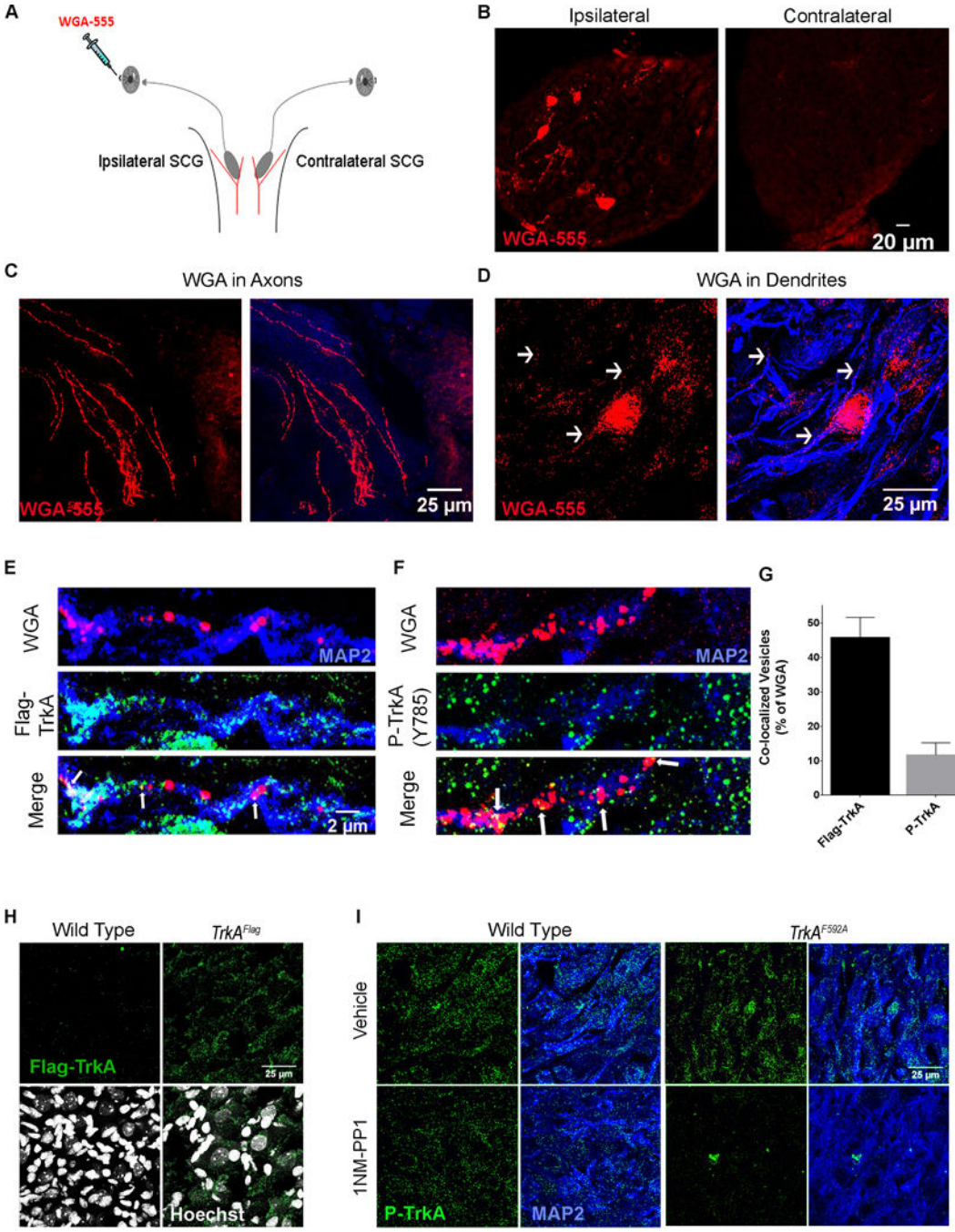

Figure 4. Distal axon-derived, signaling competent TrkA endosomes are localized within sympathetic neuron dendrites *in vivo*

A. Schematic of the assay used to track retrograde vesicle transport from the ipsilateral sympathetic target field to postganglionic neuron CBs and dendrites. WGA-555 injected into the anterior chamber of the eye is endocytosed by sympathetic neuron distal axons and transported retrogradely to the CBs and dendrites of sympathetic neurons residing in the SCG; located where the carotid artery branches into internal and external branches (red). **B.** Specific WGA-555 labeling of neurons in the ipsilateral ganglion (left) but not the

contralateral (right). **C.** WGA-555 vesicles in sympathetic axons. **D.** WGA-555 vesicles in MAP2+ dendrites. **E.** Retrogradely trafficked WGA vesicles are co-localized with Flag-TrkA puncta in dendrites 16 hours post injection. **F.** Retrogradely trafficked WGA vesicles are co-localized with P-TrkA puncta in dendrites 16 hours post injection. E is same scale as F. **G.** Quantification of E and F, n=3 animals. **H.** 5 μm sections of SCG tissue immunostained for Flag-TrkA and labeled with Hoescht (bottom), showing specific Flag puncta not in wild-type (left) but only in $TrkA^{Flag}$ (right) animals. **I.** 3 μm sections of SCG tissue immunostained for P-TrkA (Y785) and MAP2 of both WT (left) and $TrkA^{F592A}$ (right) animals treated with IP injections of either vehicle (top) or 1NMPP1 (bottom). There is specific reduction of P-TrkA puncta in 1NMPP1 treated $TrkA^{F592A}$ but not control animals. Data are presented as mean ± SEM. See also Figure S3.

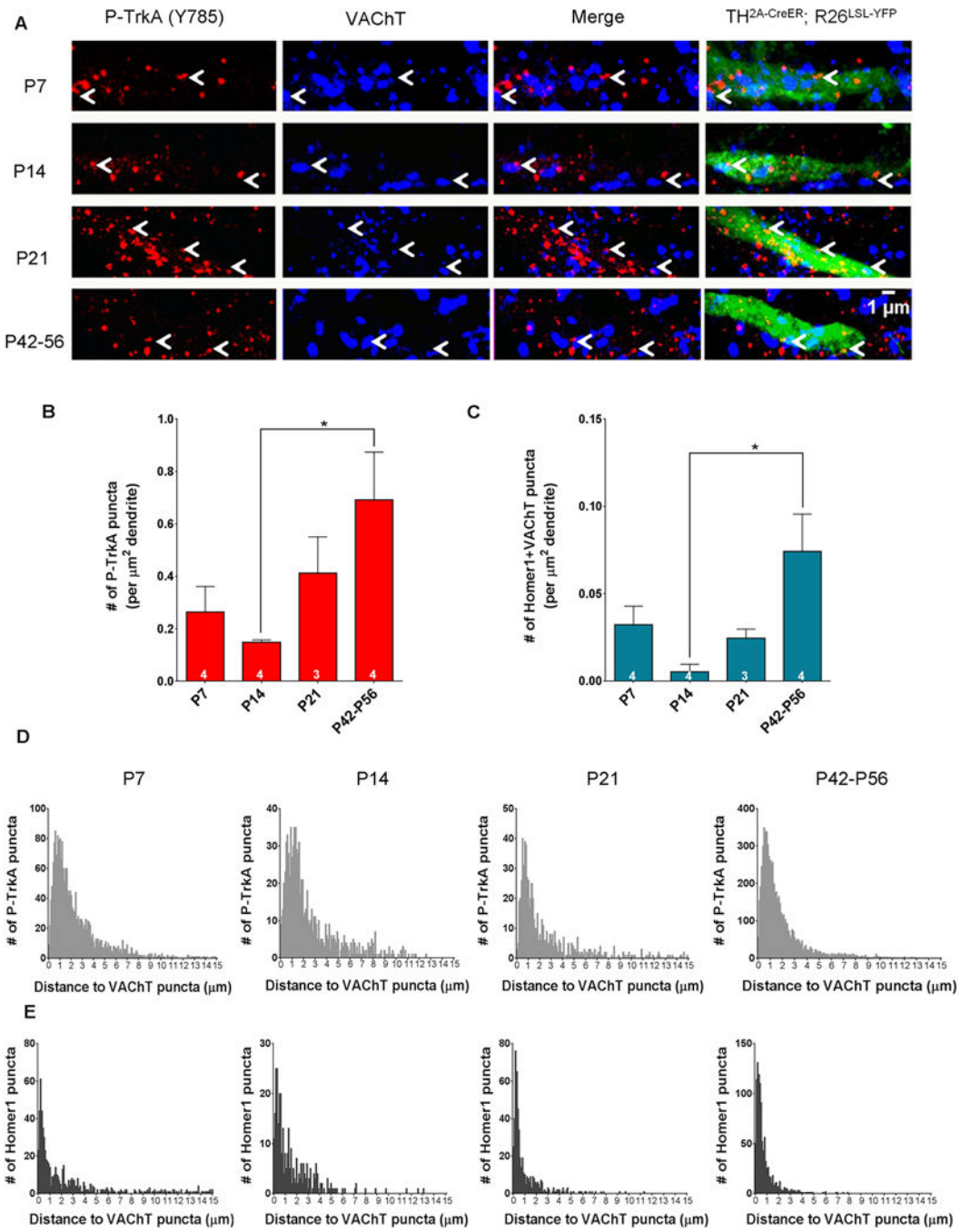

Figure 5. TrkA signaling endosomes are found in dendrites and in close proximity to synapses throughout development *in vivo*

A. Dendrites of *TH*$^{2A\text{-}CreER}$;*R26*$^{LSL\text{-}YFP}$ (Ai3) sparsely labeled cells in the SCG at developmental time-points P7, P14, P21 and P42–P56 immunostained for P-TrkA (Y785) (left) and VAChT (left middle). Arrowheads denote P-TrkA (Y785) puncta found in dendrites close to VAChT puncta. **B.** Quantification of the number of P-TrkA puncta per µm^2 of labeled dendrite. One way ANOVA $F(3, 11) = 3.845$ $P<0.05$ *post hoc* Tukey's multiple comparisons' test: *$p<0.05$. **C.** Quantification of the number of co-localized

Homer1 and VAChT puncta per μm^2 of labeled dendrite. One way ANOVA $F(3, 11) = 5.147$ $P<0.05$ *post hoc* Tukey's multiple comparisons' test: *$p<0.05$. **D.** Histograms of the distance between P-TrkA puncta and the nearest VAChT puncta within labeled dendrites. **E.** Histograms of the distance between Homer1 puncta and their nearest VAChT puncta within labeled dendrites. D, E bin size is 0.1 μm. Data are presented as mean ± SEM. See also Figure S4.

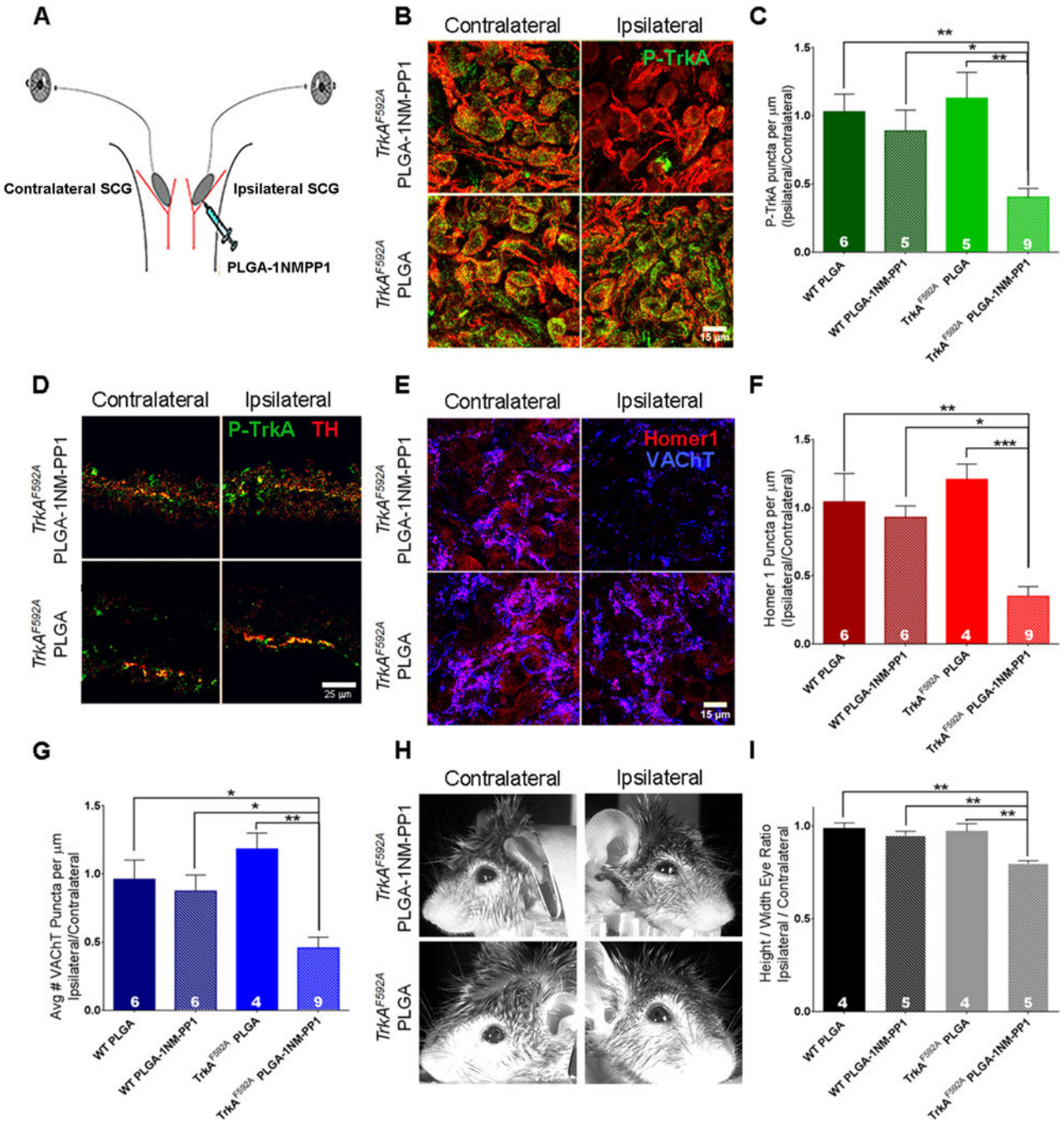

Figure 6. Somatodendritic TrkA kinase inhibition results in decreased synaptic puncta in the SCG

A. Schematic of the assay used to inhibit TrkA signaling in the somatodendritic compartment of postganglionic neurons *in vivo:* injection of 1NMPP1 loaded PLGA micropsheres into one (ipsilateral) SCG of *TrkA*^{F592A} mice. All analyses were performed 6–8 hours after injection. **B.** Reduction of P-TrkA puncta in the injected ganglion (right), but not the contralateral ganglion (left) of *TrkA*^{F592A} mice. No changes of P-TrkA level was observed in *TrkA*^{F592A} mice injected with control PLGA microspheres. **C.** Quantification of

number of ipsilateral P-TrkA puncta compared to number of contralateral P-TrkA puncta in PLGA microsphere or PLGA-1NMPP1 microsphere injected *TrkA*^{F592A} and wild-type (WT) mice. One way ANOVA F (3, 21) = 8.091 P<0.001 *post hoc* Tukey's multiple comparisons' test: *p<0.05. **D.** Similar level of P-TrkA (Y785) staining in TH+ sympathetic axons innervating the iris was observed in both contralateral (left) and ipsilateral (right) target fields in *TrkA*^{F592A} mice injected with either PLGA microspheres or PLGA-1NMPP1 microspheres. E. Reduction of VAChT and Homer1 puncta in the ipsilateral ganglion (right), but not the contralateral ganglion (left) of *TrkA*^{F592A} mice. **F** and **G.** Quantification of number of ipsilateral SCG Homer1 (F) and VAChT (G) puncta compared to the number of contralateral SCG Homer1 (F) and VAChT (G) puncta in either PLGA microsphere or PLGA-1NMPP1 microsphere injected *TrkA*^{F592A} and WT mice. Homer1: One way ANOVA F (3, 21) = 10.06 P<0.0005 *post hoc* Tukey's multiple comparisons' test: *p<0.05. VAChT: One way ANOVA F (3, 21) = 10.06 P<0.005 *post hoc* Tukey's multiple comparisons' test: *p<0.05. **H.** Representative images of ptosis in ipsilateral eyes compared to contralateral of PLGA microsphere or PLGA-1NMPP1 microsphere injected *TrkA*^{F592A} mice. **I.** Quantification of ptosis (ratio of height over width of the eye) comparing the ipsilateral eye to the contralateral eye. One way ANOVA F (3, 14) = 10.64 P<0.001 *post hoc* Tukey's multiple comparisons' test: *p<0.05. Data are presented as mean ± SEM. See also Figure S5.

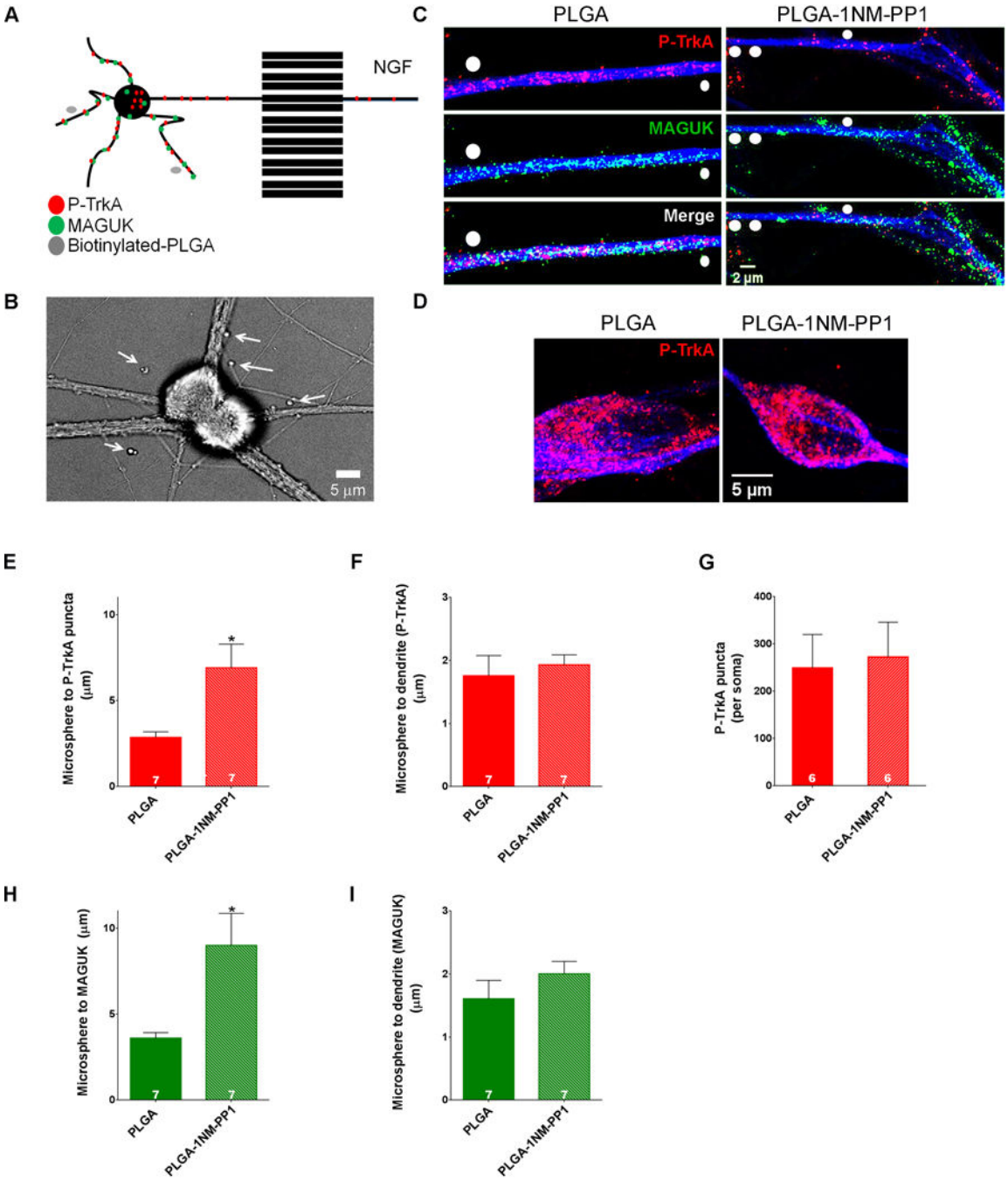

Figure 7. Distal axon-derived TrkA signals locally, within dendrites, to maintain PSDs in sympathetic neurons

A. Biotinylated-PLGA-1NMPP1 microspheres were applied to the somatodendritic compartment of DIV 14 compartmentalized *TrkA*^{F592A} sympathetic neurons cultured on coverslips pre-coated with streptavidin while NGF was applied to distal axons to achieve localized TrkA kinase inhibition pockets adjacent to dendrites. **B.** Bright field image of SCG neurons. Arrows denote PLGA-1NMPP1 microspheres. **C.** P-TrkA and MAGUK puncta in dendrites of neurons treated with PLGA (left) or PLGA-1NMPP1 (right) microspheres.

White circles are drawn over microspheres. **D.** P-TrkA puncta in soma of neurons treated with PLGA (left) or PLGA-1NMPP1 (right) microspheres, quantified in **G. E and H.** Quantification of the distance between PLGA or PLGA-1NMPP1 microspheres and the nearest P-TrkA (D) or MAGUK (G) puncta; Welch's t-test*$p<0.05$. **F and I.** Quantification of the distance between each PLGA microsphere and dendrite mask per experiment. Data are presented as mean ± SEM. See also Figure S6.